Title
Extracting More Information from the Existing Freeway Traffic Monitoring Infrastructure

Author
Coifman, Benjamin

Publication Date
2006-05-01

CALIFORNIA PATH PROGRAM
INSTITUTE OF TRANSPORTATION STUDIES
UNIVERSITY OF CALIFORNIA, BERKELEY

Extracting More Information from the Existing Freeway Traffic Monitoring Infrastructure

Benjamin Coifman
The Ohio State University

California PATH Research Report
UCB-ITS-PRR-2006-10

This work was performed as part of the California PATH Program of the University of California, in cooperation with the State of California Business, Transportation, and Housing Agency, Department of Transportation, and the United States Department of Transportation, Federal Highway Administration.

Final Report for Task Order 5302

May 2006

ISSN 1055-1425

Extracting More Information from the Existing Freeway Traffic Monitoring Infrastructure

TO 5302 Final Report

Dr. Benjamin Coifman
Associate Professor
The Ohio State University
Department of Civil and Environmental Engineering and Geodetic Science
Department of Electrical and Computer Engineering
2070 Neil Ave
Hitchcock Hall 470
Columbus, OH 43210
V: (614) 292-4282
F: (614) 292-3780
E: Coifman.1@OSU.edu

Abstract:

This report presents the results of TO 5302, Extracting More Information from the Existing Freeway Traffic Monitoring Infrastructure. This report represents significant advances in the PATH sponsored research into vehicle reidentification from conventional loop detectors, first by extending the methodology across major merge and diverge freeway sections. Second, it extends the methodology to single loop detectors. The report also extends the understanding of traffic phenomena impacting both traffic flow and the performance of the reidentification algorithms. It examines the impacts of lane change maneuvers on delay and develops a model to capture these impacts.

Keywords:

Freeway traffic monitoring, vehicle reidentification, travel time measurement, lane change maneuvers, traffic flow theory.

EXECUTIVE SUMMARY

This report presents the results of TO 5302, Extracting More Information from the Existing Freeway Traffic Monitoring Infrastructure. This report represents significant advances in the PATH sponsored research into vehicle reidentification from conventional loop detectors and examines the impacts of lane change maneuvers on traveler delay.

The most important task of a traffic surveillance system is to reliably determine whether a facility is free flowing or congested. Conventional vehicle detectors are capable of monitoring discrete points along the roadway but do not provide information about conditions on the link between detectors. This new information would be useful to the operating agencies for taking timely decisions in response to various delay causing events and hence reduce the resulting congestion of the system. This paper presents an approach that matches vehicle measurements between detector stations to provide information on the conditions in the link rather than relying on the point measurements from the detectors. This work reidentifies vehicle measurements using the existing loop detector infrastructure and extends earlier efforts, adding the ability to match vehicles across major diverges and merges. The examples include a case where the reidentification algorithm responded to delay between two detector stations an hour before the delay was locally observable at either of the stations used for reidentification. While the previous work was limited to dual loop detectors, the present effort extends the methodology to single loop detectors; thereby making it more widely applicable. Although the research uses loop detector data, it would be equally applicable to data obtained from any other traffic detector that provides a reproducible vehicle feature.

The report then shifts attention to the impacts of lane change maneuvers. Freeway traffic congestion and associated delays have become a serious problem over much of the world. Considerable effort has been made to study different factors that could cause traffic delays. Among these factors it is suspected that Lane Change Maneuvers (LCMs) could be one source of traffic delay. Little empirical research has been done on this topic although the lane changing process is very common on multilane roadway segments. This fact arises from two main difficulties: first, it is difficult to differentiate the changes in delay caused by LCMs from that of the preexisting delay caused by a queue. Second, it is difficult to quantify LCMs since it requires both spatial and temporal coverage. This paper presents the concept of delay caused by LCMs and proposes a method to estimate it within a given lane relative to the situation in which no LCMs had taken place. This estimation method enables us to investigate the impact of LCMs on traffic delays based on vehicle trajectory data, which record the time and location of each vehicle at each instant. The preliminary study shows the effectiveness of the proposed method to estimate delays caused by LCMs and reveals how LCMs impact delays on congested freeway segments.

Finally this report seeks to apply the LCM developments. A recent paper by Newell proposed a simplified car-following theory based on a novel logic. The basic assumption for this theory is that spacing and vehicle velocity are linearly related. Several other researchers studying wave speeds through the traffic stream have since found empirical evidence supporting Newell's simplified car-following theory. However, these earlier efforts have not explicitly verified the aforementioned basic assumption and in fact they have found that Newell's theory fails in the presence of frequent lane change maneuvers without providing detailed analyses. Taking a different approach, our paper studies the spacing velocity relationship using vehicle trajectory data collected during congestion, upstream of an on-ramp, where lane changing is infrequent. The empirical results show that a lane change maneuver perturbs the linear spacing velocity relationship. However, despite the disturbances from lane change maneuvers, the assumption of the linear relationship between spacing and velocity is reasonable most of the time for the vehicles on the study segment. The empirical results of this study have implications for most other car-following theories as well.

TABLE OF CONTENTS

LIST OF FIGURES

LIST OF TABLES

1 OVERVIEW

Because travel time provides information over an extended freeway link, rather than at a single point, it is a key parameter for ATIS applications and it is a powerful tool for ATMS. Under PATH sponsorship, we have already developed a prototype travel time measurement system that utilizes existing dual loop speed traps and "model 170" controllers. This research has advanced the work by improving the vehicle reidentification algorithms (Section 2), then examines the impacts of one of the major confounding factors, lane change maneuvers (Section 3), and finally uses the insights to better model these impacts (Section 4).

2 VEHICLE REIDENTIFICATION AND TRAVEL TIME MEASUREMENT ACROSS FREEWAY JUNCTIONS USING THE EXISTING DETECTOR INFRASTRUCTURE

2.1 Introduction

The most important task of a traffic surveillance system is to reliably determine whether a facility is free flowing or congested. Conventional vehicle detectors are capable of monitoring discrete points along the roadway but do not provide information about conditions on the link between detectors. This new information would be useful to the operating agencies for taking timely decisions in response to various delay causing events and hence reduce the resulting congestion of the system. This paper presents an approach that matches vehicle measurements between detector stations to provide information on the conditions in the link rather than relying on the point measurements from the detectors. As has already been demonstrated by Coifman (2003), the starting point for this section, vehicle reidentification can be used to detect the onset of congestion rapidly over a freeway link using the existing detector infrastructure. This work holds the same objective, but sets out to develop a more robust algorithm than the earlier effort. The most significant difference between the present work and the earlier effort is that the present research does not limit vehicle reidentification to only one lane, which allows vehicle reidentification even when the candidate vehicle changes lanes. The improved detection allows for reidentification across major merges or diverges in the freeway segment, where one cannot assume that most vehicles travel along the same lane. The examples include a case where the reidentification algorithm responded to delay between two detector stations an hour before the delay was locally observable at either of the stations used for reidentification. While the previous work was limited to dual loop detectors, the present effort extends the methodology to single loop detectors; thereby making it more widely applicable. Although the research uses loop detector data, it would be equally applicable to data obtained from any other traffic detector that provides a reproducible vehicle feature.

The basic idea behind the work is to identify 'distinct' vehicles at the downstream detector station, and for each of these vehicles, try to find a matching measurement from the same vehicle in the data from the upstream detector station. The travel time for traversing the distance between the two detector stations can be found by subtracting the times at which a matched vehicle was observed. After accounting for noisy measurements, if the travel times of matched vehicles fall inside a time window that represents free flow travel time, the link is considered to be in free flow conditions, otherwise the link is considered to be congested. The algorithm can report link travel times from free flow conditions down to an average link velocity of 20 mph, ensuring that normally one or more delayed vehicles will be detected when delays occur.

Other vehicle reidentification methods use vehicle signatures from video cameras (e.g., MacCarley, 2001; Huang and Russell, 1997), the much more detailed inductive signature from new loop detector sensors (e.g., Kuhne and Immes, 1993), and Automatic Vehicle Identification, all of which require new hardware. This cost aspect makes this study very relevant as the benefits of this study are two fold; first, it will allow further evaluation of the value of information obtained from vehicle reidentification and second, if successful, it may prove to be an inexpensive means of obtaining these data.

The next section presents the analysis, starting with the processing used to measure vehicle lengths and a discussion of distinct vehicles that are easier to identify in the vehicle fleet. Then, the section presents the reidentification methodology. Next, results are presented in detail from several freeway segments. Finally, it closes with the conclusions of the research.

2.2 Analysis

2.2.1 Data from Loop Detectors

The data available from a conventional dual loop detector is sparse, though nonetheless, much of the information is discarded in conventional aggregation. Rather than aggregating vehicle measurements together, we measure individual vehicle lengths. Figure 2-1A shows a time-space diagram for a vehicle passing over a dual loop detector. The dual loop detector has two detection zones as indicated in the figure. Figure 2-1B shows the transitions recorded by the controller, (on_1, on_2) and (off_1, off_2), the turn-on and turn-off times at each of the loops, respectively. These measurements are used to calculate dual-loop traversal times using the rising edges TT_r, dual-loop traversal time using the falling edges TT_f, the on-time for the first loop OT_1 and the on-time for the second loop OT_2, as shown in the figure.

For vehicles passing over a dual loop, the length of the vehicle is proportional to the on-time and inversely proportional to the traversal time. The length measurements are subject to resolution constraints of OT_i and TT_i, which in turn depend on the vehicle velocity, the sampling rate of the detectors and separation between the loops. Since the reidentification algorithm explicitly compares measurements of each vehicle between stations, it must accommodate these measurement limitations. To this end, a length range that has sufficient tolerance is developed. At the same time, since the algorithm seeks to match the length measurement of a given vehicle detected at the downstream station to the same vehicle detected at the upstream station, the length range aims to increase the probability of intersection between the length ranges of the 'true' upstream and downstream matches while minimizing false positives as much as possible when the measurements

do not come from the same vehicle. The following length estimates were used to define the length range.

$$\text{Length estimate \#1: } L1 = S*OT_1/TT_r \tag{2-1}$$

$$\text{Length estimate \#2: } L2 = S*OT_2/TT_f \tag{2-2}$$

$$\text{Length range} = [\text{Min}(L1,L2), \text{Max}(L1,L2)] \tag{2-3}$$

where S is the loop separation in m.

2.2.2 Importance of Long Vehicles

In most cases long vehicles constitute a small percentage of the vehicle fleet that travels through the freeway. To illustrate this point, Figure 2-2 shows the cumulative distribution of measured vehicle lengths observed over 24 hours at one freeway detector station. It can be seen that fewer than 10 percent of the observations range from 7 m (23 ft) to 24.4 m (80 ft). The long vehicles thus are a 'distinct' category of vehicles. Because the long vehicles encompass a large range of feasible lengths and they normally pass with a lower frequency, it makes them easier to differentiate from one another than it is for most vehicles. This section uses vehicles that are longer than a threshold based on the 90th percentile length for all the vehicles passing a loop detector over 24 hours. In all of the analyses that follow, only long vehicles are considered unless otherwise noted.

In each lane at a downstream station, the long vehicles are subsampled out from the rest of the fleet using this threshold, namely, if

$$d_l > D_{threshold} \tag{2-4}$$

where, d_l is the lower bound of the length range of the vehicle measured at downstream station, and $D_{threshold}$ is the minimum threshold length of long vehicles. The long vehicles are then numbered consecutively based on their arrival order.

2.2.3 Comparison of Length Ranges and Travel Time Representation

Each long vehicle at the downstream station is considered the primary vehicle with a set of candidate vehicles that are feasible matches at the upstream station. This choice of terminology reflects the fact that as soon as a vehicle passes the downstream station we know that if there is a match at the upstream station it has already been observed. The upstream vehicle candidates include all vehicles

(no length threshold) and are chosen using the two following rules: a candidate must arrive at the upstream station before the arrival of the primary vehicle at the downstream station to ensure positive travel time, and the total number of candidates shall not exceed the jam density of link, i.e., the storage capacity, n. The length range of the primary vehicle is compared with candidate vehicles present within the n most recent upstream station arrivals as determined by the jam density.

The length range from Equation 2-3 captures measurement uncertainty. So the length range upstream should intersect the length range downstream if the two measurements came from the same vehicle. Of course many other candidate vehicles will have a length range that intersects that of the primary vehicle. Formalizing this concept, denoting the upper and lower bounds from Equation 2-3 for the primary vehicle as d_h and d_l, and similarly the bounds for each candidate vehicle as u_h and u_l. a primary vehicle candidate pair is considered a possible match if,

$$u_h \geq d_l \text{ and } d_h \geq u_l \tag{2-5}$$

The possible matches for each primary vehicle are then stored in matrix format indexed by travel time, where the travel time for each matched pair is obtained by subtracting the arrival time of the possible matche at the upstream station from the arrival time of the given primary vehicle at the downstream station. The rows of this Travel Time Matrix (TTM) correspond to the primary vehicle number. The indices of the columns of the matrix represent the possible travel times rounded to the nearest integer second. The TTM is populated with 0's except for the travel times for each of the given primary vehicle's possible matches, which are given a value of 1. To avoid a very large column size and thereby improve computational efficiency, the size of TTM is constrained by link velocities falling between 2 mph and 90 mph. Figure 2-3 shows a hypothetical matrix with primary vehicle numbers indexing the rows and travel times in seconds the columns. Some cells are highlighted, representing the pairs that have been found by matching. For example, Cell (K,T) that has been highlighted represents the downstream vehicle 'K' has a corresponding upstream match that yields a link travel time of 'T' seconds.

2.2.4 Extracting Information from the Travel Time Matrix

The travel time trends over the link during free flow and moderately congested conditions are readily evident in the TTM because the link travel time of the true matches of consecutive vehicles fall in a small range and occur with relatively high density, while the false positives are randomly distributed with lower density. Similarly, vehicles that arrive within a very short time of each other at the downstream station normally have similar link travel times. These trends extend to the moderately congested periods but are not clearly discernible during heavily congested periods due

to the large range of the travel times. For example, if link velocity drops from 10 mph to 5 mph, the link travel time will double. Extracting these trends from the TTM reduces of the number of possible matches and point to the most probable matches. To this end the algorithm tries to identify the dense areas of the TTM that would capture the trend exhibited in the TTM. As discussed below, the TTM matrix is transformed to the maximum density matrix (MDM), to identify the dense areas. In the first step, to accommodate the fact that successive vehicles may experience slightly different travel times, the possible travel times are extended horizontally to adjacent cells using the following equation,

$$f\left(TTM(K,T)\right) = \begin{cases} 1, & \sum_{H=T-p}^{T+p} TTM(K,H) > 0 \\ 0, & \text{otherwise} \end{cases} \tag{2-6}$$

This function f() gives a weight of 1 to a cell if any of the adjacent 'p' cells in the same row of TTM had a value of 1. The value of p is set to 8mph, half of the expected difference in travel times during free flow periods. Next, the MDM is generated recursively using the following equation,

$$MDM(K,T) = \sum_{R=K-1}^{K-q} MDM(R,T) + f\left(TTM(K,T)\right) \tag{2-7}$$

where, K corresponds to downstream vehicle number, T corresponds to link travel time yielded by a potential match of vehicle K. The first term of Equation 2-7 is the sum of the cells in the same column of the previous q rows, so a cell in the MDM gets more weight if preceding vehicles also had the same travel time. The value of 'q' is set to be the number of long vehicles that arrived at the downstream station within the previous 5 minutes with the maximum allowed value of q set at 25. These thresholds make sure that vehicles that passed the downstream station much before the current vehicle do not influence the current extraction of the vehicle's link velocity. Unlike the TTM, which has a value of '1' for cells that correspond to a primary vehicle number-travel time pair, the MDM will exceed 1 for the densest areas because of the summation in Equation 2-7. Figure 2-4B shows an example of the MDM superimposed on the original TTM.

The MDM is then subsampled to pull out a new matrix, MDM_{20}. First, the column corresponding to the maximum value in each row of the MDM is found. These cells are given a value of 1 in MDM_{20} while all other cells in that row of MDM_{20} are assigned a value of zero. MDM_{20} is then truncated so that all columns with a link velocity slower than 20 mph are unilaterally set to zero to exclude these slower link velocities. When the link velocity is above 20mph, the densest cells of each row in the TTM should normally fall within the non-zero range of MDM_{20}. The travel times

corresponding to these cells are henceforth called the most probable travel times (MPTT). The final non-unique set of most probable matches is obtained by finding the vehicles that are responsible for these travel times. Since one is not guaranteed an intersection between the densest areas of MDM and TTM, for every primary vehicle the MPTT are compared with the travel times resulting from the initial set of primary vehicle-candidate pairs. If there is a single intersection, that pair is then considered to be a most probable match and stored. It is possible that sometimes there might not be an intersection, especially when the link velocity has fallen below the velocity bounds. In cases where there is no intersection, any pair whose absolute travel time difference with the MPTT for that primary vehicle is not greater than 1/8th of the travel time difference between upper bound and lower bound of assumed free flow velocity range is considered a most probable match and stored, i.e., if

$$\left|MPTT - TT_x\right| \le \frac{1}{8}\left(TT_{ffl} - TT_{ffu}\right) \tag{2-8}$$

where TT_x is a candidate travel time, TT_{ffl} and TT_{ffu} are the lower and upper bound on free flow travel times (65 mph and 45 mph, respectively). The value of 1/8 was arrived at empirically for reducing the number of false positives that resulted from this approach. The pair corresponding to TT_x is then retained as the MPTT for that downstream vehicle. This method for looking for matches increases the number of vehicles found by including those matches that might be slightly slower or faster than the densest areas.

2.2.5 Unique Matches

In the final set of MPTT, it is possible for a primary vehicle to have more than 1 match and a candidate vehicle to be matched with more than 1 primary vehicle. To address this issue, the matched vehicle pairs are subjected to a two-step filtering process that results in, at most, one unique match for every matched downstream vehicle. The first step is to remove any potential match that has an improbably fast link velocity based on the posted speed limit, e.g., the filtering threshold is 80 mph for a link whose posted speed limit is 65 mph in order to accommodate drivers that travel faster than the posted speed limit. In the second step, for every primary vehicle with more than one candidate vehicle match, the match that yields the median of the possible link velocities from the set of matches is accepted arbitrarily if there is an odd number matches, or the one immediately below the median velocity is chosen if there is an even number of matches. In either case, all the other entries of that vehicle are removed. Figure 2-4C shows the MPTT superimposed on the original TTM.

2.2.6 Multi Lane Vehicle Reidentification

The primary difference between the single lane case described above and the multi lane case described below is that in the multi lane case the first step is to combine the vehicles from all relevant lanes and then assign numbers consecutively according to their arrival times while also retaining the individual lane vehicle number for reference. The vehicle lengths and length ranges are calculated as explained in the single lane case. It should be noted that the number of upstream vehicles to be used for comparison with each downstream vehicle would be higher in the multi lane case because the storage density of the lanes that have been combined should be taken into consideration.

The travel time representation and extraction of information are the same as the single lane case. After finding the final unique matches, the vehicle numbers are transformed back to the original lane number. Unlike the single lane case, the multi lane case provides matches for long vehicles that changed lanes.

2.2.7 Extending to Single Loop Detectors

Unlike dual loop detectors, a single loop detector only measures each vehicle once, yielding on-time, but velocity can only be estimated in single loop detectors. Conventional velocity estimation from single loop detectors is very noisy because the assumption of a fixed average vehicle length that may or may not be representative of a given sample. Earlier work by our group has shown that different data processing at a single loop detector can make its performance to approach the accuracy of a dual loop detector, i.e., estimating the median velocity rather than the mean (Coifman et al, 2003a). The vehicle lengths are then obtained by multiplying the on-time of each vehicle by the estimated velocity.

$$\text{Estimated Length} = \text{on-time} * \text{Estimated median velocity} \tag{2-9}$$

This earlier work showed that when the estimated velocity of the sample was greater than 20 mph the average error in estimated length was less than six percent for the vehicle set considered. However, Coifman et al (2003a) notes that the error in the length estimates is expected to increase in periods with heavy truck flows. Fortunately, heavy truck flows are not common in most periods when vehicle reidentification would be of greatest interest and hence the above formula for estimation of length from single loop detectors was used. If truck flows are of concern one could use more sophisticated velocity estimation algorithms, e.g., Neelisetty and Coifman (2004). Since there is only one length estimate, the length range is modified to the following:

$$\text{Length range} = [0.8*\text{Estimated Length}, 1.2*\text{Estimated Length}] \quad (2\text{-}10)$$

The values 0.8 and 1.2 are used to give the lengths a reasonable tolerance and thereby increase the accuracy and percentage of vehicle reidentification. The 20 percent threshold was arrived at by trial and error. For an estimated length of 20 feet, the above definition would give a tolerance of 8 feet, while an estimated length of 80 feet it would yield a tolerance of 32 feet. In all of the subsequent analysis, Equation 2-3 was used for the dual loop length range and Equation 2-10 was used for single loops. The rest of the processing was identical under the two conditions.

2.3 Results

2.3.1 Dual Loop Detectors

The multi lane vehicle reidentification algorithm was implemented over different sections of the Berkeley Highway Laboratory (BHL) (Coifman et al, 2000). Figure 2-5 shows a schematic of a 0.91 mi section of westbound I-80 between station 2 and station 5. All lanes had dual loop detectors and there were two intervening stations that were not used in the vehicle reidentification. Figure 2-6 shows an example of the results of the vehicle reidentification algorithm on the section using data from July 15, 2003. Vehicles from lane 3 of the downstream station (5) were matched with vehicles from lanes 2, 3 and 4 of the upstream station (2). The figure shows the resulting link velocities for matched vehicles superimposed on the time series local velocity measurements at each of the detector stations. In this figure, it is evident that during free flow periods the long vehicles travel a little slower than the average vehicle

The BHL includes several ramps, but it does not include any major freeway merges or diverges. Moving to the I-71 freeway corridor in Columbus, OH, Figure 2-7 shows a schematic of a 0.97 mi section of southbound I-71 between stations 108 and 103. The section has 2 merges and 2 diverges including the I-71/I-70 interchange. Both stations 108 and 103 in the southbound direction have dual loop detectors. Figure 2-8 shows an example of the results of the vehicle reidentification algorithm on the section using data from May 29, 2003. Vehicles in lane 2 of the downstream station (103) were matched with vehicles from lanes 2 and 3 of the upstream station (108). Again the link velocities of the matches obtained through the vehicle reidentification algorithm over 21 hrs are shown in the figure, superimposed on the time series local velocity measurements at each of the detector stations. In fact Figure 2-4 shows a portion of the TTM, MDM and MPTT from these stations on this day. Figure 2-8 also shows the measured travel times from two probe vehicle trips through the corridor, as measured by an on-board global positioning system (GPS) receiver.

Figure 2-9 shows a schematic of a 0.95 mi section of northbound I-71 between stations 105 and 109. The section crosses the I-71/I-70 interchange in the opposite direction from the previous example. Both stations 105 and 109 in the northbound direction have dual loop detectors. Figure 2-10 shows an example of the results of the vehicle reidentification algorithm on the section using data from February 28, 2002. Vehicles in lane 2 of the downstream station (109) were matched with vehicles from lanes 1 and 2 of the upstream station (105). In this case four probe vehicle travel time measurements through the corridor were recorded throughout the day. The most significant feature of this plot is the fact that the vehicle reidentification responded to delays between 7:00 and 9:00 that were not observable at either station used in the reidentification (105 or 109). This delay is evident at the intermediate stations, e.g., station 107 shown in the plot and one of the probe vehicle runs. In the afternoon the stations at either end of the link eventually become congested, but again, the vehicle reidentification algorithm responded almost an hour before the delay was observable at either of the stations (again the delay is evident at the intermediate station not used in reidentification).

2.3.2 Single Loop Detectors

The previous examples used the dual loop data, in contrast, this section limits the input to a single loop from each of the dual loop detectors. For example, using this single loop data Figure 2-11 shows the results of reidentification between stations 105 and 109 on the same day and section shown with dual loops in Figure 2-9. So this new figure shows the resulting travel time when matching observations from the single loop detector data in lane 2 of station 109 matched with single loop detector data in lanes 1 and 2 of station 105. It can be seen that the algorithm works quite well using the single loop detector data, although the number of matches has decreased slightly. Again, the reidentification algorithm found the delay between the stations long before it was locally evident at either end of the link. One difference however was that a higher threshold of 25 ft was used for defining long vehicles when the single loop detector data from the I-71 corridor was used. Note that in this figure the estimated velocities at the detector stations are somewhat noisy before 5:00, this fact arose due to normal early morning low flow conditions and can be addressed with an occupancy filter (Jain and Coifman, 2005). Figure 2-12 shows the results of applying the vehicle reidentification algorithm to the single loop detector data from lane 2 between stations 106 and station 107 in the I-71 northbound corridor. The distance between the stations is about 0.39 mi, shown in Figure 2-9.

Table 2-1 presents the reidentification statistics for the dual loop detector data, while Table 2-2 presents the reidentification statistics for the single loop detector data. The reidentification

percentage from the single loop detector data is less than the dual loop detector data for the 0.95 mi link (I–71 Northbound 105 to 109). The percentage of reidentified vehicles from the single loop detectors increases when the link distance is less, as seen from the results in Table 2-2.

2.4 Conclusions

Conventional vehicle detectors are capable of monitoring discrete points along the roadway but do not provide information about conditions on the link between detectors. This section developed a robust vehicle reidentification algorithm to quantify conditions between detector stations. The distinct vehicles were key to this reidentification, namely the long vehicles in this case.

The reidentification results were used to find link travel times until link velocity dropped below 20 mph. About 40 percent of long vehicles were consistently reidentified over links on the order of 1 mi long using dual loop detector data, and a slightly lower reidentification rate when using single loop detector data. The travel time measurements obtained from the reidentified vehicles will be useful for studying the traffic conditions in the freeways. This work advances our earlier efforts significantly. First, the ability to match vehicles between single loop detector stations opens up additional roadways for analysis. But the most important contribution of the new algorithm is the fact that the present research does not limit vehicle reidentification to only one lane, which allows vehicle reidentification even when the candidate vehicle changes lanes. The improved detection allows for reidentification across major merges or diverges in the freeway segment, where one cannot assume that most vehicles travel along the same lane. Two out of the three links examined included a major merge and major diverge of two interstate freeways. The examples include a case where the reidentification algorithm responded to delay between two detector stations an hour before the delay was locally observable at either of the stations used for reidentification.

This analysis can be used to provide recommendations on future funding decisions for investment on expensive new infrastructure for travel time measurement, focusing resources only on freeways that promise to show an improvement in operations due to provision of travel time information. The new information would be useful to the operating agencies for taking timely decisions in response to various delay causing events and hence reduce the resulting congestion of the system. Finally, although the research uses loop detector data, it would be equally applicable to data obtained from any other traffic detector that provides a reproducible vehicle feature.

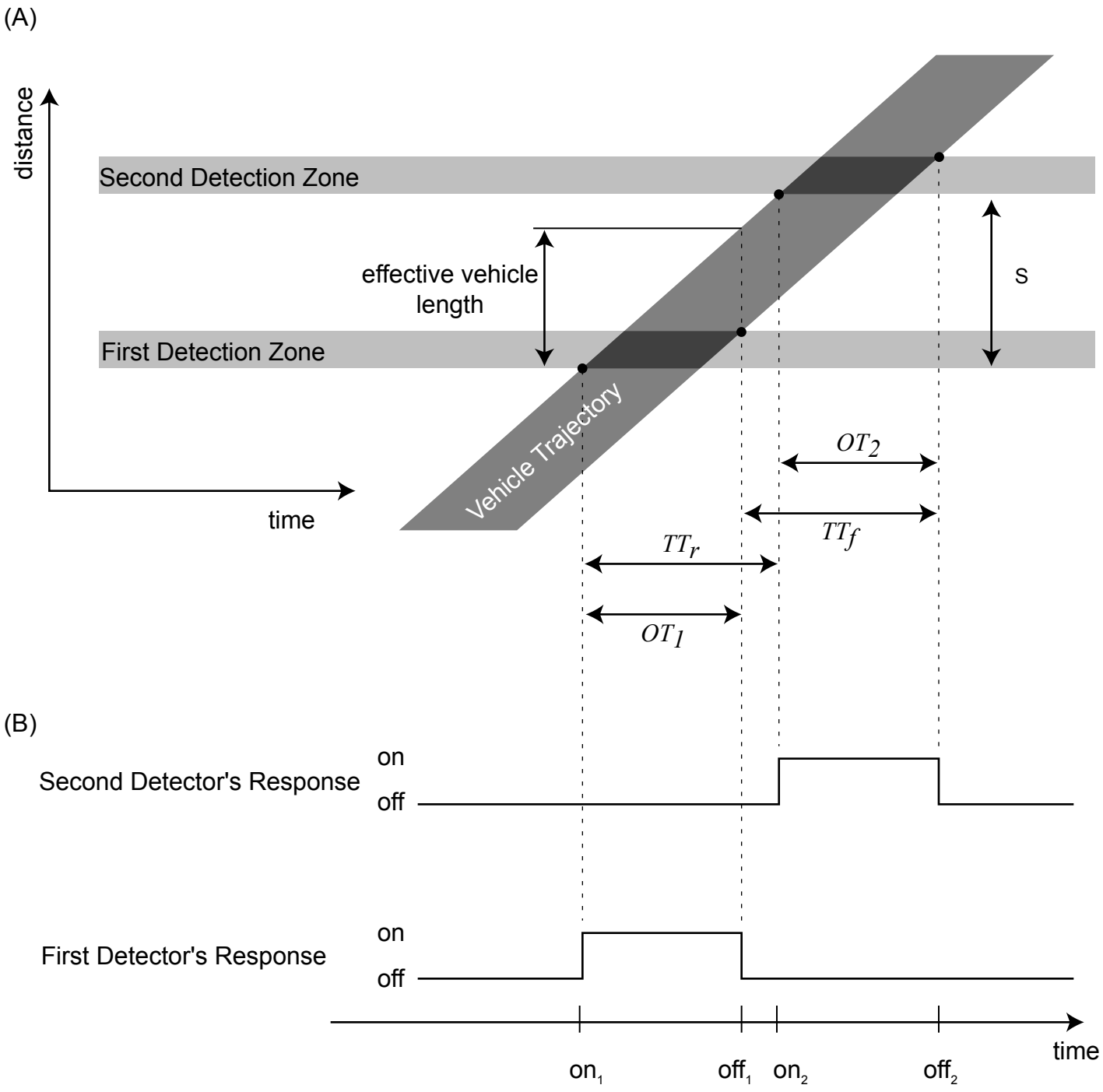

Figure 2-1, One vehicle passing over a dual-loop-detector, (A) the two detection zones and the vehicle trajectory as shown in the time space plane. (B) The associated turn-on and turn-off transitions at each detector.

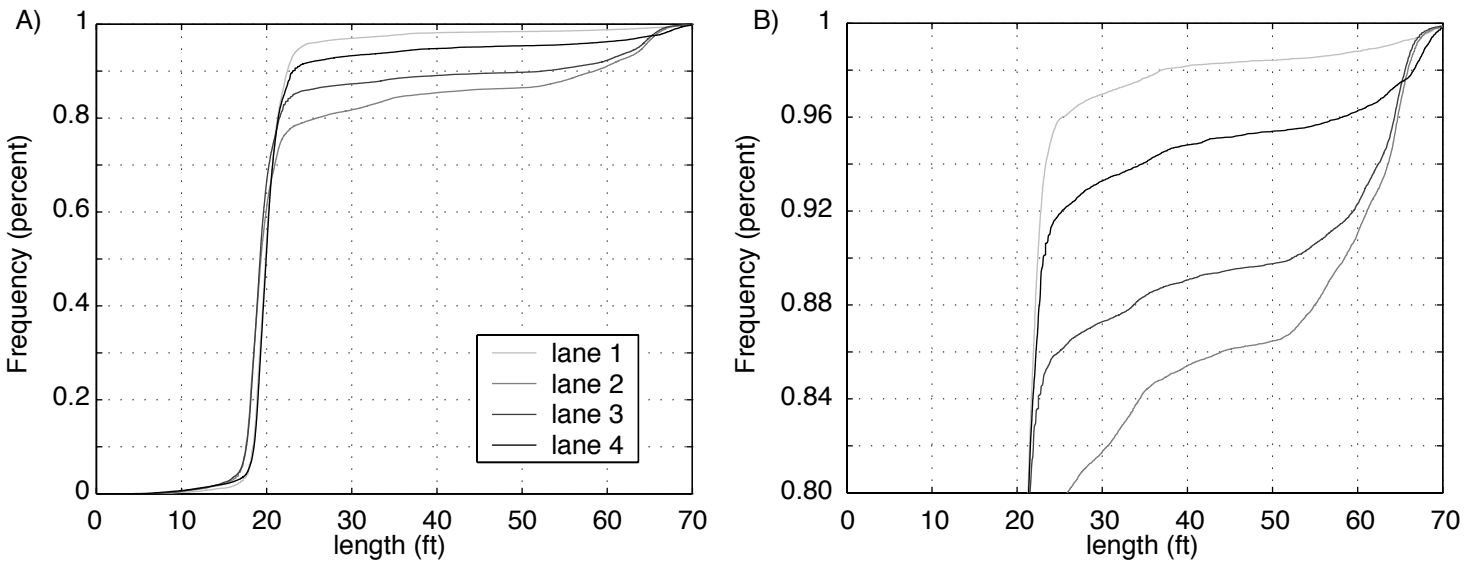

Figure 2-2, (A) Cumulative Distribution of lengths over 24 hours from one freeway detector station on I71, (B) Detail of Part A

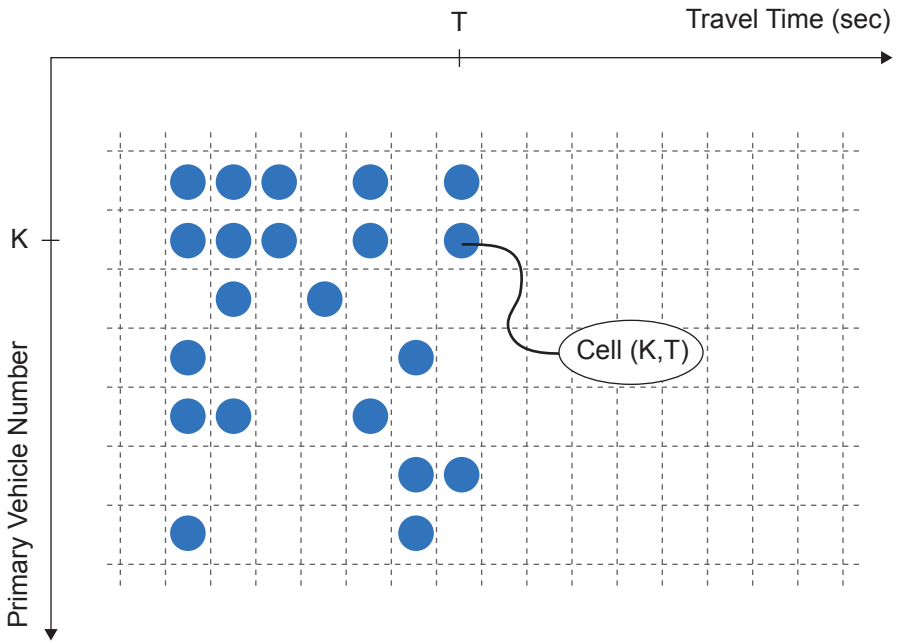

Figure 2-3, Schematic representation of a hypothetical travel time matrix.

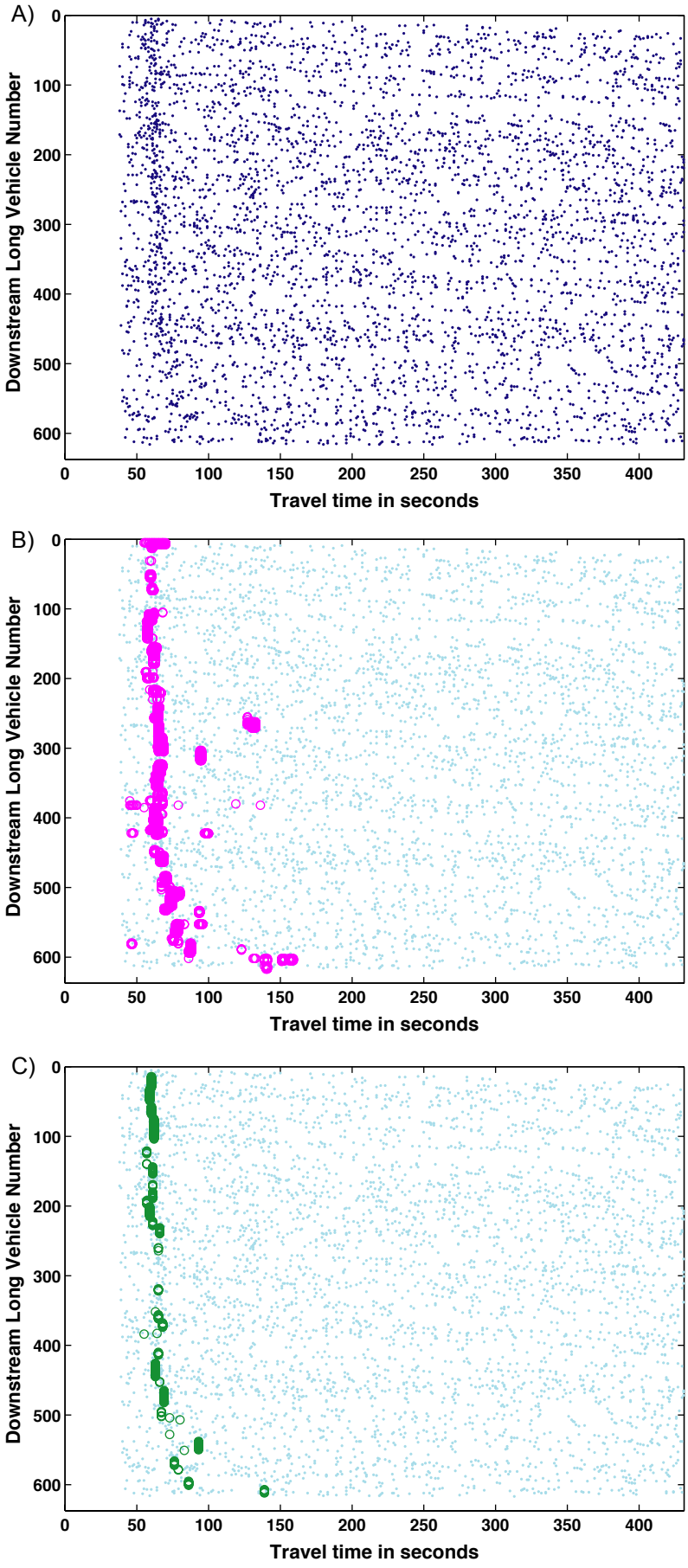

Figure 2-4, (A) Original TTM for a sample data set from two stations almost one mile apart, (B) MDM superimposed on the TTM from A, (C) MPTT after finding the unique matches superimposed on the same TTM.

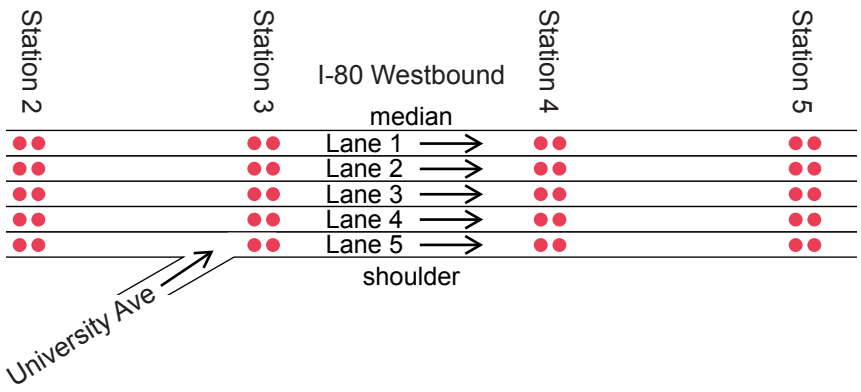

Figure 2-5, Schematic of the section between station 2 and station 5 in the westbound I-80 corridor (not to scale).

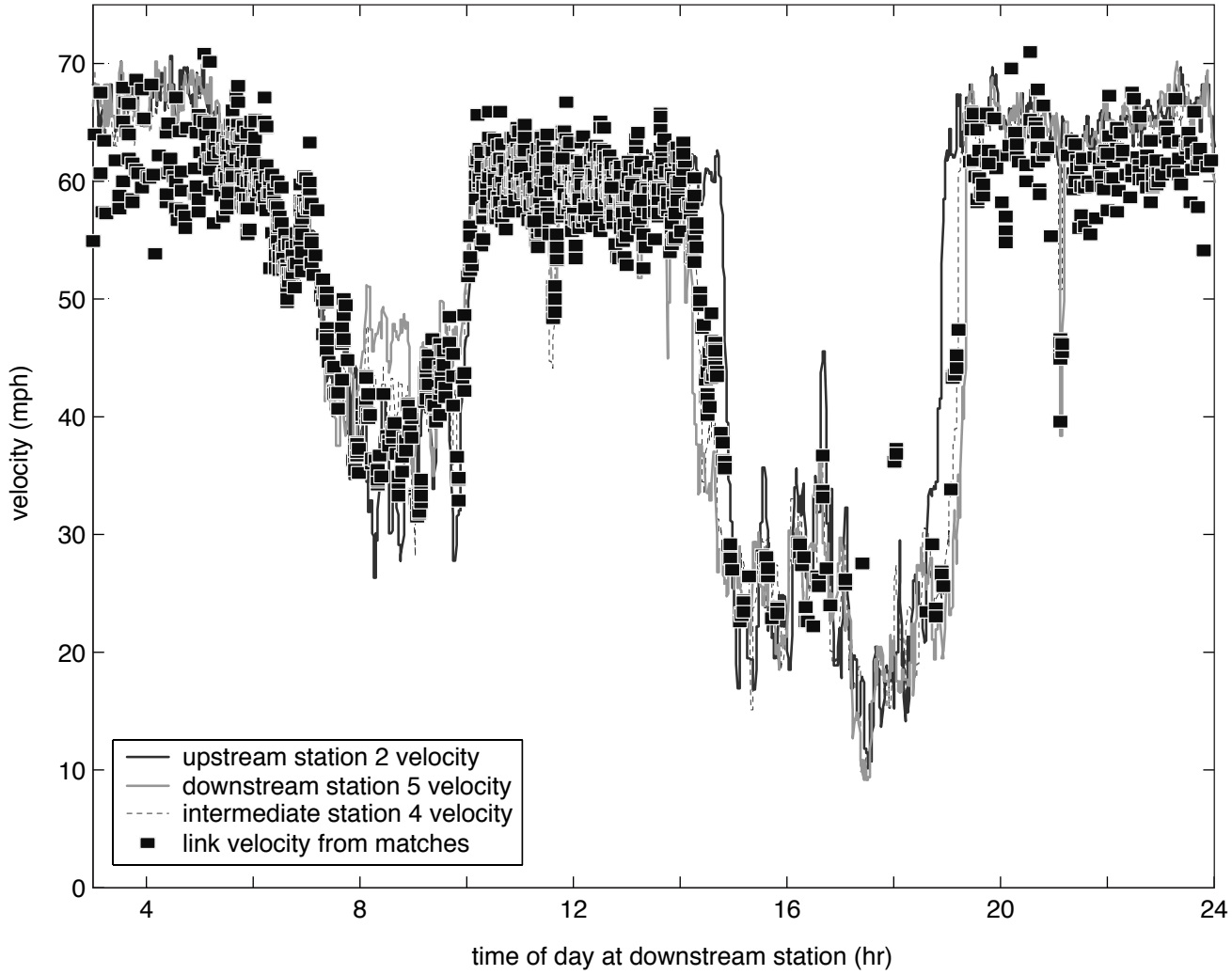

Figure 2-6, Results of vehicle reidentification between lane 3 at station 5 and lane 2, 3 and 4 at station 2 on the westbound I-80 corridor.

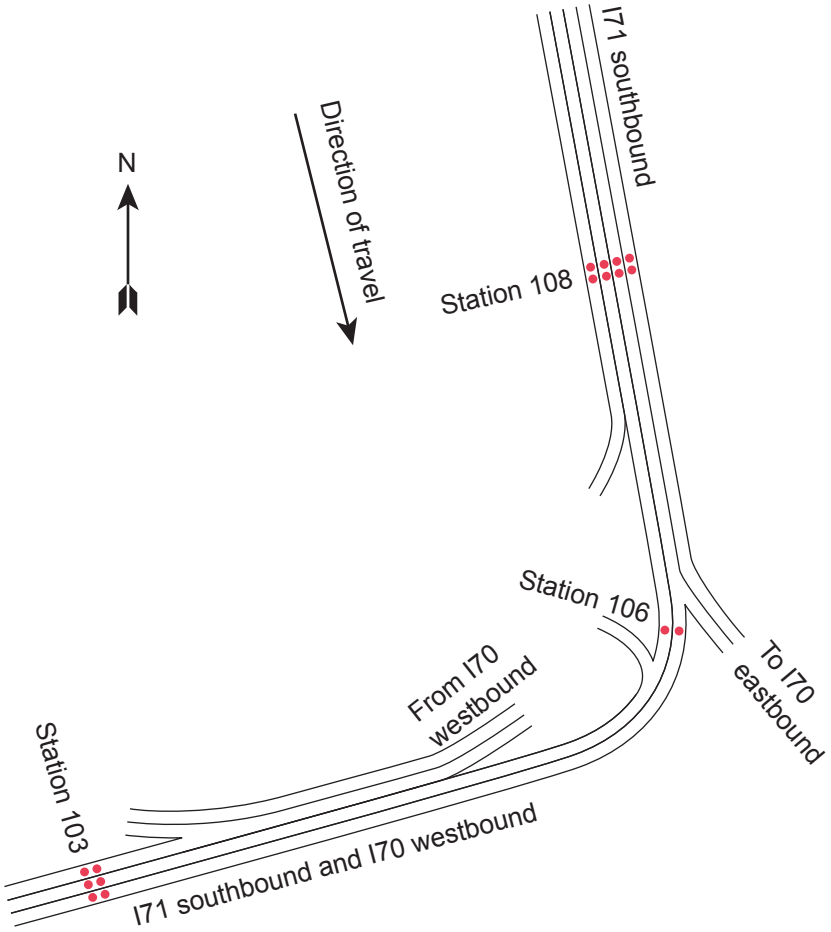

Figure 2-7, Schematic of the section between station 108 and station 103 in the southbound I-71 corridor (not to scale).

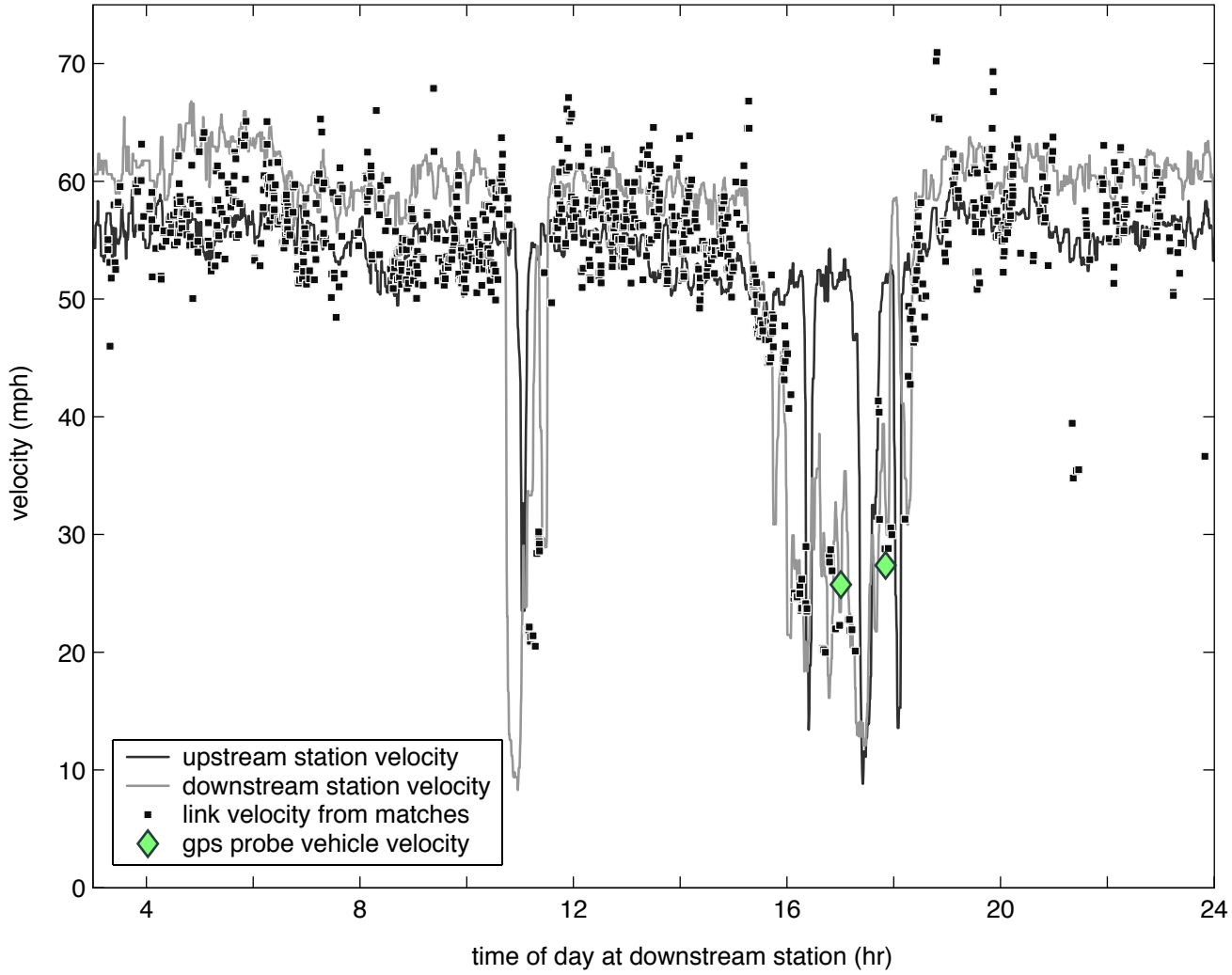

Figure 2-8, Results of vehicle reidentification between lane 2 at station 103 and lane 2 and 3 at station 108 on the southbound I-71 corridor.

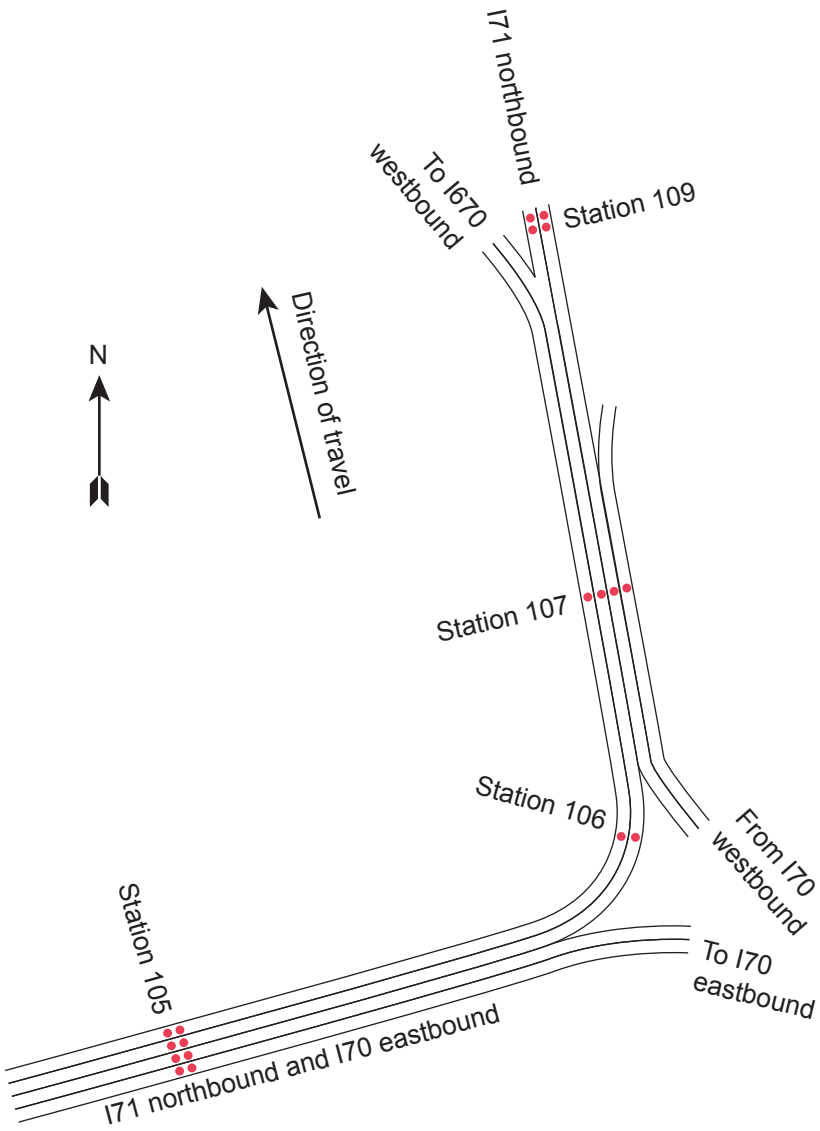

Figure 2-9, Schematic of the section between station 105 and station 109 in the northbound I-71 corridor (not to scale).

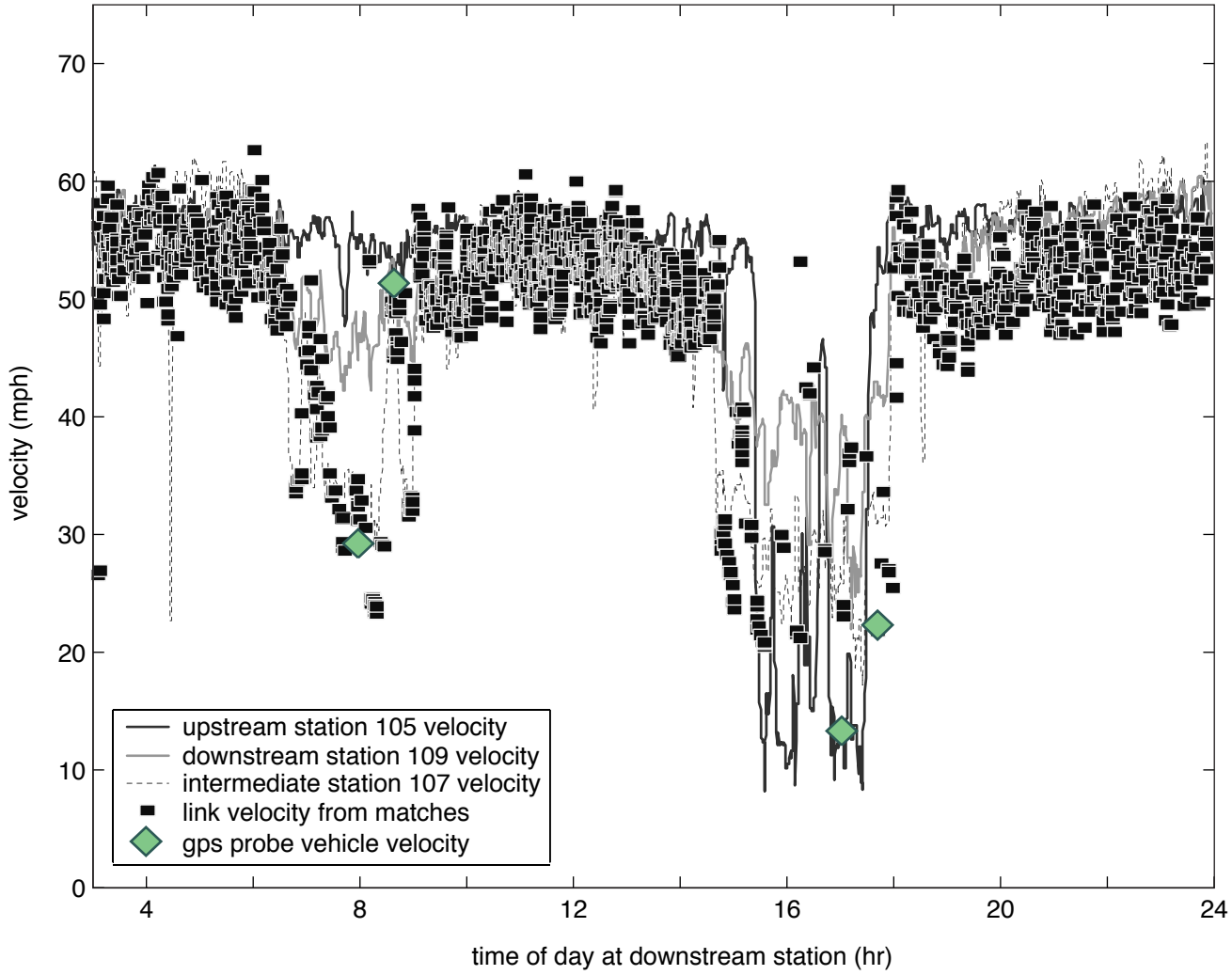

Figure 2-10, Results of vehicle reidentification between lane 2 at station 109 and lane 1 and 2 at station 105 on the northbound I-71 corridor using dual loop data.

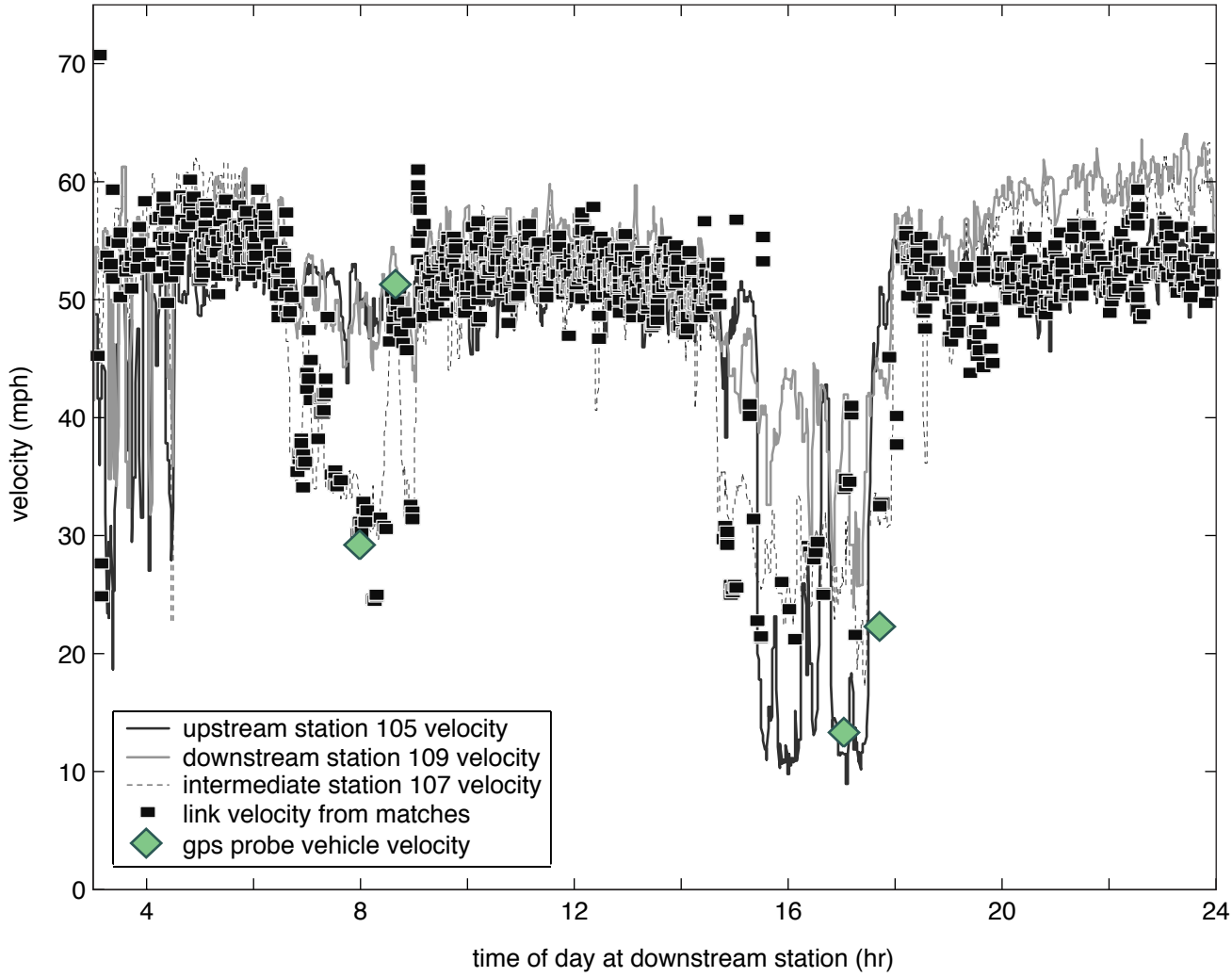

Figure 2-11, Results of vehicle reidentification between lane 2 at station 109 and lane 1 and 2 at station 105 on the northbound I-71 corridor using single loop data.

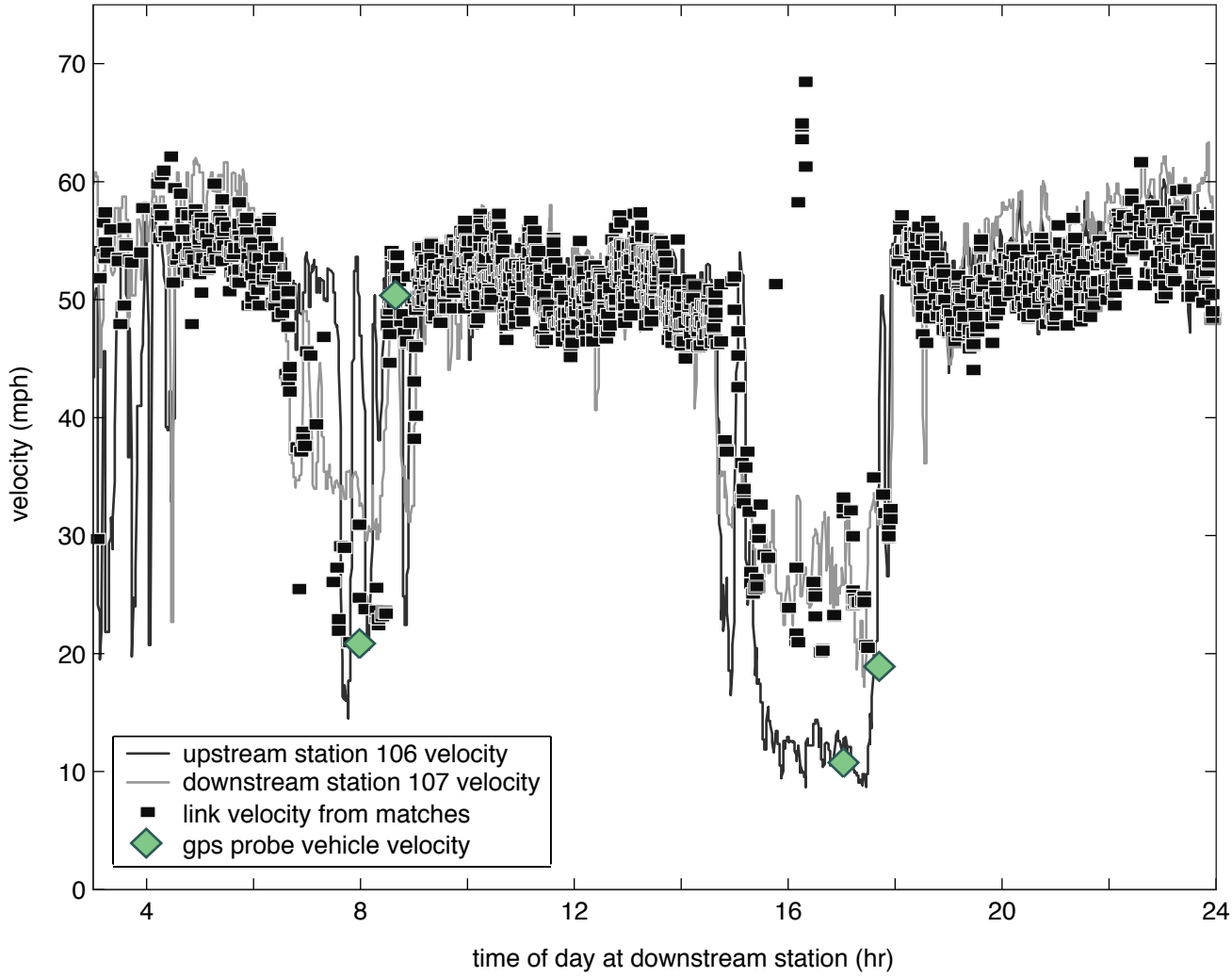

Figure 2-12, Results of vehicle reidentification between lane 2 at station 107 and lane 2 at station 106 on the northbound I-71 corridor using single loop data.

Table 2-1, Reidentification results between 0300-2400 hrs from dual loop detectors

Case	Facility		Upstream	Downstream	Distance (miles)	Total No vehicles downstream	Total No of long vehicles downstream	Total No of vehicles reidentified	% of long vehicles reidentified
1d	I-80 westbound	July 15, 2003	station 2, lanes (2,3,4)	station 5, lane (3)	0.91	26,095	3,533	1,277	36%
2d	I-71 southbound	May 29, 2003	station 108, lanes (2,3)	station 103, lane (2)	0.97	28,668	4,254	1,548	36%
3d	I-71 northbound	February 22, 2002	station 105, lanes (1,2)	station 109, lane (2)	0.95	33,960	4,430	1,809	41%

Table 2-2, Reidentification results between 0300-2400 hrs from single loop detectors

Case	Facility		Upstream	Downstream	Distance (miles)	Total No vehicles downstream	Total No of long vehicles downstream	Total No of vehicles reidentified	% of long vehicles reidentified
3s	I-71 northbound	February 22, 2002	station 105, lanes (1,2)	station 109, lane (2)	0.95	33,960	4,430	1,284	30%
4s	I-71 northbound	February 22, 2002	station 106, lane (2)	station 107, lane (2)	0.39	29,060	4,371	1,579	36%

3 A PILOT STUDY INTO THE IMPACTS OF LANE CHANGE MANEUVERS ON CONGESTED FREEWAY SEGMENT DELAYS

3.1 Introduction

Freeway traffic congestion and associated delays have become a serious problem over much of the world. Considerable effort has been made to study different factors that cause traffic delays. Among these factors, it is suspected that Lane Change Maneuvers (LCMs) could be one source of traffic delays.

To understand this conjecture, first consider a single LCM during congestion. For a vehicle that changes from origin lane A to destination lane B, it exits the former and enters the latter. Intuitively, "during very high flow or queued conditions, each entering vehicle would delay the following driver and these delays would propagate upstream" (Coifman et al, 2003b). The extent of this influence depends on how fast the resulting disturbance propagates and whether it will dissipate before the end of the queue. On the other hand, each exiting vehicle should make it possible for the following drivers in the origin lane to accelerate and reduce their delays. This disturbance would also propagate upstream. So each LCM is expected to induce two contrary effects, causing delay in the lane the vehicle enters and reducing delay in the lane the vehicle leaves. However, the addition in delay caused by an entering vehicle might be greater than the savings in delay by an exiting vehicle in congested traffic conditions. On congested freeway segments, if vehicle i forces its way into lane B from lane A, the vehicle that will be following vehicle i in lane B has to decelerate immediately to avoid collision, the deceleration is mandatory. However, the following vehicle in lane A does not necessary have to accelerate immediately and take the advantage of the larger gap left by vehicle i, the acceleration is discretionary. In addition to this imbalance in the effects of entering and exiting vehicle on traffic delay, there are also likely transient effects arising from the fact that the vehicle will simultaneously occupy two lanes during the process of changing lanes, momentarily decreasing the capacity of the link. This latter feature becomes particularly important near bottlenecks, potentially reducing throughput.

Although the lane changing process is very common on multilane roadway segments, little research has been done on the possible delays caused by LCMs. Previous research on LCMs either developed models to study the interrelations between the traffic conditions and the frequency (or fraction) of vehicles changing lanes (e.g., Gazis et al, 1962; Munjal and Pipes, 1971; Michalopoulos and Beskos, 1984; Worrall and Bullen, 1970; Sheu, 1999; Sheu and Ritchie, 2001), or specified lane changing rules and applied these rules in traffic simulation (Gipps, 1986 ; ang and Koutsopoulos, 1996; Ahmed et al, 1996; Zhang et al, 1998; Hidas, 2002; Wei et al, 2000; Toledo et

al, 2003). The published research is lacking in empirical studies investigating the concept of delays caused by LCMs explicitly, due to two main difficulties. First, it is difficult to differentiate the delay caused by LCMs from the preexisting delay caused by a queue. Second, it is difficult to quantify LCMs since it requires both spatial and temporal coverage.

This section presents the concept of delay caused by LCMs and proposes a method to estimate it within a given lane. The basic idea is to estimate delay caused by LCMs as the difference of the measured travel time and the estimated travel time assuming that there had been no LCMs. Vehicle trajectory data are employed in this section. Since the location of each vehicle at each second is known from the trajectory data, it is trivial to calculate the measured travel time and to quantify LCMs, i.e., to find the time and location of each LCM. This preliminary study shows the effectiveness of the proposed method to estimate delays caused by LCMs. It also reveals how LCMs would impact delays on congested freeway segments. Although there are some limitations in this pilot study, the results motivate further research on the effects of LCMs and help the understanding of the factors contributing to delay, which could be used in evaluating the necessity of lane management strategies in areas of frequent LCMs, such as weaving sections. Such study also has the potential to be used to quantify LCMs since it models the relationship between LCMs and delays caused by LCMs.

This section is organized as follows. First, a method to estimate delay caused by LCMs and a method to study the impact of LCMs on delays are introduced. Next, the two methodologies are applied based on a set of trajectory data collected from California. Finally, the section closes with a discussion of the findings, limitations, and future research.

3.2 Methodology

The first task to study delay caused by LCMs is to quantify it. It is proposed that this delay be computed as the difference of the measured and estimated travel time. The measured travel time can be easily obtained from trajectory data or Vehicle Reidentification Algorithms, which match the observations of a given vehicle from two locations in space, e.g., MacCarley (1998), Izumi et al (2000), Hellinga (2001), Coifman (1998), Coifman and Cassidy (2002), and Coifman (2003). In this section the estimated travel time should reflect conditions in the lane if there had been no LCMs, this approach can employ the travel time estimation algorithm proposed by Coifman (2002). This algorithm was initially proposed to estimate the expected travel time from a dual loop detector and is briefly described in the first subsection below. However, as will be shown in the second subsection, such estimation algorithm can also serve to estimate the expected travel time had there been no LCMs. The third subsection presents the method to study the impacts of LCMs on delays.

3.2.1 Travel Time Estimation Algorithm

The travel time estimation algorithm (Coifman, 2002) assumes that during congestion signals and waves propagate upstream at some constant velocity (u_c) and remain unchanged over the entire segment; every vehicle that passes a detector station reflects the continually evolving traffic state. Although the constant wave velocity assumption is not perfect, this assumption has been supported by several studies (Newell, 2002; Newell, 1993; Hall and Gunter, 1986; Banks, 1989; Cassidy, 1998; Cassidy and Mauch, 2001; Mauch and Cassidy, 2002; Windover and Cassidy, 2001; Coifman and Wang, 2005), both theoretical and empirical.

Vehicle speeds and arrival times are recorded at the detector station and can be represented in a time-space plot. A chord in the time-space plane is defined to be the straight line passing the location of the detector at the instant the vehicle passes with a slope equal to the vehicle's measured speed. The hypothetical example in Figure 3-1 shows the chords for vehicle i to $i+5$ at the detector station during congestion. A chord provides a rough approximation of vehicle trajectory for a short distance downstream of the detector station. During congested conditions the model assumes the change in traffic state between two vehicles is small and the evolving state can be approximated by the discrete observations when vehicles pass. Given u_c, the interfaces between the discrete states are parallel signals (dashed lines in Figure 3-1) reaching the detector station each time a vehicle passes and all vehicles encountering a signal will make the same traffic state transition. Since the chord of vehicle i intersects the signal that later reaches the detector at instant t_i^{i+1}, vehicle i changes its speed to that dictated by the signal, as detected at the station when vehicle $i+1$ passes. Vehicle i will travel at this speed until it reaches another observed signal. Iterating this procedure, the estimated trajectory of vehicle i can be constructed as the bold line in Figure 3-1. The estimated travel time between the detector station and any specific location D would be the difference of the passage times at two locations based on the estimated trajectory. Using this algorithm, each vehicle is assumed to follow the same trajectory as the vehicle ahead of it, shifted in space and time, which coincides with the model proposed by Newell (2002).

This method can also be applied upstream of a detector station, with the speed of vehicle i updated by the detected speeds of vehicles preceding (instead of following) vehicle i. So, the travel time between two stations can be estimated from either end: using the observed data at the downstream station to estimate conditions on the link upstream of that station, $TT_{est}^{d/s}$, or using the observed data from the upstream station for conditions on the link downstream of that station, $TT_{est}^{u/s}$. Both estimates are for the same link, but come from separate data at one end or the other, allowing for a

comparison to catch detector errors. In this study $TT_{est}^{d/s}$ is employed for reasons discussed in the Pilot Study Based on Field Data section below. The identification of detector errors is addressed in detail in Coifman (2002).

3.2.2 Method to estimate delays caused by LCMs

To understand how the travel time estimation algorithm produces an estimate assuming there are no LCMs, it is worthwhile to first consider how LCMs influence vehicle travel times. The hypothetical example in Figure 3-2A shows the trajectories of seven vehicles in the same lane during congestion. To simplify the problem, all vehicles are assumed to travel with speed $V1$ most of the time. There are detector stations on either end of the subject link, labeled upstream and downstream. All vehicles pass both stations in the lane except vehicle a3, which enters the subject lane between the two stations from another lane. Under congested traffic conditions, vehicle a4 has to decelerate from $V1$ to $V2$ to accommodate the entrance of a3 ahead. The transition between traffic states of $V1$ and $V2$ induces a signal propagating upstream. After a3 finishes the LCM and there is acceptable headway between a3 and a4, the latter vehicle resumes car following and accelerates to travel with an average speed $V1$ to match the vehicle ahead of it. This transition generates another signal propagating upstream, parallel to the previous one.

If there were no LCMs, all vehicles (except a3) would traverse two stations within time $t1$ as illustrated in Figure 3-2A. As a result of the LCM of a3, vehicles a4, a5 and a6 will travel with speed $V2$ for some distance while between the two stations. The travel time for vehicle a4 is extended to $t2$ as shown in Figure 3-2A, i.e., it encounters a delay of $t2 - t1$ caused by the LCM, in which $t2$ is the measured travel time of vehicle a4 and $t1$ is the estimated travel time assuming there are no LCMs. The sum of delays for a4, a5 and a6 would be the total delay within the link caused by the LCM of a3. A similar example for an exiting vehicle is shown in Figure 3-2B, where the expected travel time should be longer than the measured travel time, indicating that an exiting vehicle allows its following vehicle traverse the link faster than otherwise expected.

In both examples the estimated travel time based on the observed data at the downstream station, $TT_{est}^{d/s}$, produces an estimate of travel time without the influence of LCMs, $t1$, for all seven vehicles since the disturbance of the LCM of a3 propagates upstream and was not observable at the downstream station. On the other hand, the estimated travel time based on the observed data at the upstream station, $TT_{est}^{u/s}$, is an estimate including the influence of LCMs, $t2$, for all seven vehicles. In either case, the travel time is estimated correctly for some vehicles and incorrectly for others.

To formulize the above analysis, the delay caused by LCMs for each vehicle can be estimated as follows:

$$Delay_{LCM} = TT_{measured} - TT_{est}^{d/s} \quad (3\text{-}1)$$

Where, $Delay_{LCM}$ is delay attributed to LCMs, and $TT_{measured}$ is the measured travel time.

In reality, the trajectories in Figure 3-2A and 3-2B would not be straight lines and they are not necessarily parallel. Likewise, the detected speeds at the downstream station would not all be identical. It is not clear how long the disturbance generated by the LCM could propagate and how it is related to the traffic conditions such as density. The approach assumes that a LCM occurs at a point but the following vehicle's accommodation occurs over some distance, e.g., a4 traveling at V2 in Figure 3-2A. When a LCM occurs just downstream of a detector it is possible that most of the accommodation actually occurs upstream of the detector, placing the event in one link and the impact in another. There could also be detection errors at the detector stations. All of these factors add errors to Equation 3-1. Thus, it is of interest to verify the assumption that $TT_{est}^{d/s}$ captures conditions without the influence of LCMs.

3.2.3 Method to study the impact of LCMs on delays

Consider the hypothetical example in Figure 3-3. The freeway is congested between two detector stations, denoted upstream and downstream. Five vehicles pass both stations and are represented with bold lines labeled from a1 to a5 in Figure 3-3. Their travel times are available based on trajectory data. The lane changing vehicles are labeled with b1 to b4. The speed of the backward moving signals is assumed to be constant at u_c and an upstream moving signal passing through vehicle a5 as it crosses the upstream detector is represented by a dashed line. Thus, $TT_{est}^{d/s}$ employs the traffic state along line segment AB to estimate travel time along AC assuming no LCMs take place within triangle ABC while $TT_{measured}$ reflects conditions experienced by a vehicle traveling along trajectory AC to measure travel time directly and as a result capturing the effects of any LCMs.

Vehicle a5 passes the upstream station at time t_2 and the downstream station at time t_4. During this period, it passes through the signals emanating from LCMs ahead of it. In the absence of any LCM, all signals that influence the progression of a5 through the link would pass the downstream station after t_5, the downstream station passage time of the signal that eventually meets a5 at the upstream

station at t_2. LCM signals emanating to the left of the line BC in Figure 3-3, such as that from vehicle b1, are not expected to influence the travel time of a5 between the two stations since such signals reach vehicle a5 outside of the two stations. Signals emanating from LCMs downstream of both stations in Figure 3-3, such as the LCM signal from vehicle b2, would influence the travel time of a5 between the two stations but this signal would pass both stations. Both $TT_{est}^{d/s}$ and $TT_{measured}$ would include the influence from vehicle b2 and the difference on the right side of Equation 3-1 is not expected to contain such influence. LCM signals emanating within the triangle ABC in Figure 3-3, such as that from vehicle b3, would influence the travel time of a5 between the two stations but not the estimated travel time based on downstream station. So the LCM of vehicle b3 contributes to the delay of vehicle a5 between the two stations as measured by Equation 3-1, and in general the delay of vehicle a5 will change in response to LCMs in the triangular time space region ABC (obviously, such delay is likely related to other traffic features as well).

To study the impact of LCMs on delays, the dependent variable is chosen to be the estimated delay caused by LCMs for each through vehicle based on Equation 3-1, and the explanatory variables include the number of LCMs in the triangular time space region ABC along with variables describing the traffic conditions. Some examples of the explanatory variables are the number of entering vehicles N_{EN}, the number of exiting vehicles N_{EX}, the net inflow (defined to be N_{EN} minus N_{EX}), density, speed, headway and flow at the upstream and downstream stations (via Edie, 1963). The effect of the numbers of entering and exiting vehicles has already been discussed above. As for the other possible explanatory variables, it is expected that as density increases, the impact of a LCM on delay is diminished since the reactions of the non-lane-changing drivers to LCMs is damped. Similarly, lower speeds have the same effect on delays for the same reason.

3.3 Pilot Study Based on Field Data

A pilot study was conducted using the above methods with vehicle trajectory data collected by Turner-Fairbank Highway Research Center (TFHRC) in June, 1983 from I-405 South Bound at Santa Monica Blvd., Los Angeles, CA (Smith, 1985). A schematic of the site is shown in Figure 3-4. The site was filmed from an aircraft flying clockwise at a slow speed. Data were reduced at one frame per second for one hour of the film. Each record contains the information of a vehicle at an instant, which includes vehicle ID, speed, lateral and longitudinal position, and lane number. Traffic was free flow for the first several minutes after which a surge in ramp volume caused the average speed in lane 1 to drop to about 20 mph and this state continued for the remainder of the dataset. Queuing in lane 1 extended upstream of the section approximately 30 minutes into the film and no

incidents affected flow in the section. The second half hour data on lane 1 were selected for the pilot study since the study is focused on LCMs in congested traffic conditions.

The travel time estimation algorithm requires the observations of time and speed at which vehicles pass the downstream station. Such data can be collected by traditional detection devices like loop detectors but cannot be directly obtained from trajectory data. So for this dataset it is necessary to specify the locations of hypothetical upstream and downstream detector stations and then interpolate the trajectory data to derive vehicle passage times and speeds at these locations. Theoretically, these stations can be placed at any location along the 1616 ft segment. To avoid the direct influence from the on-ramp and simplify the problem in this pilot study, the hypothetical upstream and downstream stations are placed at 200 ft and 800 ft respectively. Based on the trajectory from a vehicle, the passage time at the upstream station, tA , is the linear interpolation of the time of two observations just before and after the vehicle crosses the upstream station. The quotient of distance and time between these two observations is vA , the vehicle speed at the upstream station. The passage time tB and speed vB at the downstream station are similarly defined. The simulated downstream detector data are used to calculate $TT_{est}^{d/s}$ between the upstream and downstream stations, i.e., the travel time without the influence of LCMs between the stations. These estimated travel times are then used together with the measured travel times to calculate delays caused by LCMs based on Equation 3-1. As stated earlier, the wave velocity is assumed constant and a value of 10 mph is adopted in this study after calculating the wave velocity based on several different methods, including studying the generalized flow-density relationship (Edie, 1963), studying the propagation of stop waves, Newell's simplified car following model (Newell, 2002), cross correlation analysis (Wang et al, 2004), and cross spectral analysis (Wang et al, 2004). The minimum and maximum across the five estimates are 8.7 mph and 10.8 mph, respectively.

This pilot study recognized the following dependent variable and subsequently explanatory variables relative to the notation in Figure 3-3:

$Delay_{LCM}$ = estimated delay caused by LCMs defined in Equation 3-1 (seconds),

N_{EN} = number of entering vehicles in time space region ABC (vehicle),

N_{EX} = number of exiting vehicles in time space region ABC (vehicle),

V_{dn}^{a} = arithmetic mean speed (time mean speed) at downstream station over time interval AB (mile/hour),

V_{dn}^{h} = harmonic mean speed (space mean speed) at downstream station over time interval AB (mile/hour), and

K_{dn} = density at downstream station (veh/mile) defined as Q_{dn} / V_{dn}^{h}, where Q_{dn} (veh/hour) is flow at downstream station over time interval AB.

The corresponding upstream measures are not used because their measurement region only touches ABC at a point in the time space plane.

Figure 3-5 shows the scatter plots of the dependent variable $Delay_{LCM}$ and LCM related explanatory variables, N_{EN} and N_{EX}. Figure 3-5A indicates that the estimated travel time tends to be greater than the measured travel time in these data; that is, $Delay_{LCM}$ tends to be negative. Since $Delay_{LCM}$ is the estimated delay caused by LCMs and there are more exiting vehicles than entering vehicles on the subject section, as can be seen from the negative net inflows in Figure 3-5B, this result concurs with the expectation that exiting vehicles would reduce delays. Similarly in Figure 3-5B, 81% of the data points lie in the quadrant corresponding to negative delay and negative net inflow, indicating that when net inflow is negative, the estimated delay caused by LCMs tends to be negative. Figures 3-5C and 3-5D illustrate that $Delay_{LCM}$ tends to increase with N_{EN} and decrease with N_{EX}, as indicated by the estimated simple regression lines where delay is regressed against N_{EN} and N_{EX}, respectively. All of these observations lend credence to the effectiveness of the estimation method of delay caused by LCMs defined in Equation 3-1.

As a first attempt in the study of the impact of LCMs on traffic delays, basic linear regression models are estimated to capture the relationship between delay and the various explanatory variables discussed in the methodology section. More sophisticated models are left for future research.

The residual plots of the simple linear regression models, whereby one explanatory variable is considered at a time, were examined first. The results show that no transformations of N_{EN}, N_{EX} and density variables are necessary. However, the reciprocal transformation of the speed variable is more reflective of the raw data and yields a higher correlation with delay. The correlations among the explanatory variables were also computed and analyzed. As expected, density and the reciprocal of speed are highly correlated. Therefore, one of these variables is included in the model specification at a time since they relate to the same causal process as discussed in the previous section. As a result, three models are estimated. The first model only includes the primary

explanatory variables N_{EN} and N_{EX}. The second and third models add density and the reciprocal of speed, respectively, measured at the downstream station, i.e., along AB in Figure 3-3, consistent with the use of $TT_{est}^{d/s}$. The estimation results of the three model specifications are shown in Table 3-1.

In all three models, both coefficients of N_{EN} and N_{EX} are significant at the 1% level, which shows that from the statistical regression point of view they do impact $Delay_{LCM}$ on the congested freeway segment. In addition, both coefficients have the expected signs in all three models, i.e., the positive coefficient of N_{EN} implies that each entering vehicle would cause delay and the negative coefficient of N_{EX} indicates each exiting vehicle would reduce delay. In Model 2 and 3, the coefficients of the additional explanatory variables are found to be significant at the 1% level and have the expected signs.

In all three models, the constant terms are significant. For Model 1, the significant constant indicates that when there is no LCM (i.e., $N_{EN} = N_{EX} = 0$), $Delay_{LCM}$ is significantly different from 0, which is not reasonable. However, for the other models, it can be shown that when there is no LCM, on average the constant term is cancelled out by the other terms in the model. Therefore, clearly N_{EN} and N_{EX} do not explain the process entirely.

Across different models, the coefficient of N_{EN} ranges from 1.44 to 2.19 seconds, and the coefficient of N_{EX} ranges from 0.6 to 1.0 seconds. These data give some idea how much an entering vehicle would increase the delay and how much an exiting vehicle would decrease the delay in congested traffic conditions. In each of the models, hypothesis tests show that the coefficient of N_{EN} is significantly different in magnitude from that of N_{EX}, indicating that delay caused by an entering vehicle is greater than the savings in delay by an exiting vehicle in congested traffic conditions. Thus, it is not appropriate to use net inflow (i.e., $N_{EN} - N_{EX}$) as an alternate explanatory variable.

3.4 Conclusions

This section presents the concept of delay caused by LCMs and proposes a method to estimate it. The estimation result is further applied to study the impact of LCMs on delays using trajectory data. Such study should help understand traffic delay for better congestion management and further

the understanding of traffic dynamics into an important area where much remains unknown. A pilot study shows that the proposed study methods are feasible. Nevertheless, further research needs to be carried out to evaluate the impact of some of the simplifying assumptions made. Several linear regression models from this pilot study are presented and the results comply with the expectations. This section provides an empirical start for the study of LCMs impacts on delay.

There are some limitations of the work that should be addressed in the future, several of which are as follows. The proposed methodology has so far been tested only on half-hour of trajectory data from a single lane on a section just before an on-ramp. The observation data at the simulated upstream and downstream stations are interpolated from the vehicle trajectories, rather than collected from the field. In addition, the inhomogeneous geometric features of this section might have caused the low goodness-of-fit measure of the linear regression models. Identifying the impacts of inhomogeneous features is an important topic for further research and trajectory data collected from congested traffic conditions are necessary for further study.

Several assumptions and simplifications are made in this section and some of them need further verification treatment. The wave velocity was assumed to be constant, a value of 10 mph was used in the pilot study. Although not shown in this section, the value of the constant wave velocity was proven to be an important confounding factor and its value should be determined carefully, as was done herein with five different methods. In addition, this study counts the number of LCMs in the triangular time space region as ABC shown in Figure 3-3. However, this triangular region is just a simplification since some LCMs outside of this region might also contribute to the delay. For example, vehicle b4 in Figure 3-3 will not influence the travel time of vehicle a5 between the two stations and will not contribute to the delay of vehicle a5 if it is assumed that a vehicle can change its speed instantly. However, in reality vehicle a5 will need some time to accommodate the lane change of vehicle b4 and such accommodation might occur between the two stations if vehicle b4 changes lane at a spot that is very close to the line BC in Figure 3-3. Given that the numbers of entering and exiting vehicles are discrete variables, the treatment of such explanatory variables in statistically modeling delay relationships requires further attention.

One needs to both understand the operation of individual lanes and the combination of all lanes in a given direction. This section is limited to the former, when considering the impacts across all lanes. On the one hand, it remains possible that some of the effects may cancel out and become imperceptible in aggregate delay. On the other hand, an aggregate delay could still be present and detectable due to the finding in this section that the delay caused by a LCM into a lane is greater than the gain in travel time resulting from a LCM out of a lane. Moreover, because the accommodation occurs over long distances, the gain in one lane may be spatially or temporally

separated from the loss in another. Although this imbalance may be small, it could prove to be one mechanism that causes delay and disturbances (e.g., the driver behind an entering vehicle may decelerate and then accelerate to accommodate the LCM, all following vehicles will be constrained by the fluctuations in this trajectory as the impacts propagate upstream). Likewise, a vehicle momentarily consumes more capacity while straddling two lanes than it would have had it remained in a single lane. From a capacity and delay standpoint one may argue that these phenomena are only important within a bottleneck, which may prove to be true, but the understanding of LCMs within a queue should also further understanding LCMs' impacts within a bottleneck where they can impact throughput. The understanding could also lead to establishing more precisely the influence area of a bottleneck, where it begins and ends. Away from bottlenecks the work potentially has implications on safety (e.g., accidents due to stop and go traffic) and car following theory. Finally, if LCMs away from a bottleneck cause a measurable change in delay for a given lane, it could provide a tool to quantify LCMs within a queue even if LCMs do not impact the net delay across all lanes, thereby providing previously unavailable details about the flow of vehicles within a queue.

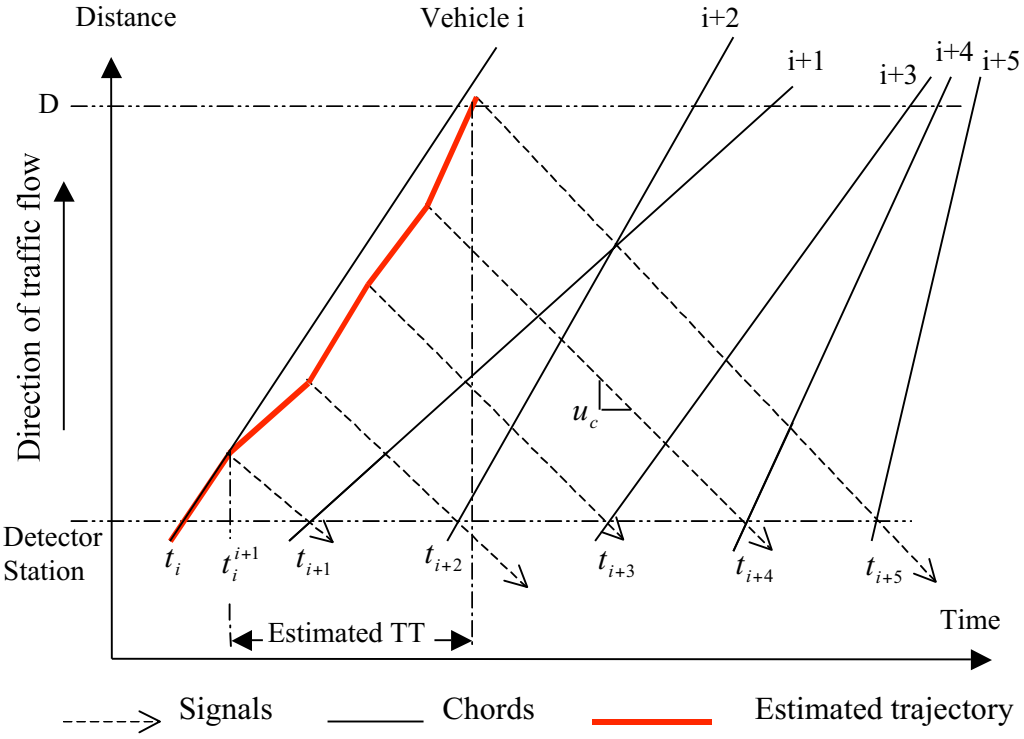

Figure 3-1 Estimated travel time and trajectory for vehicle i (adapted from Coifman, 2002).

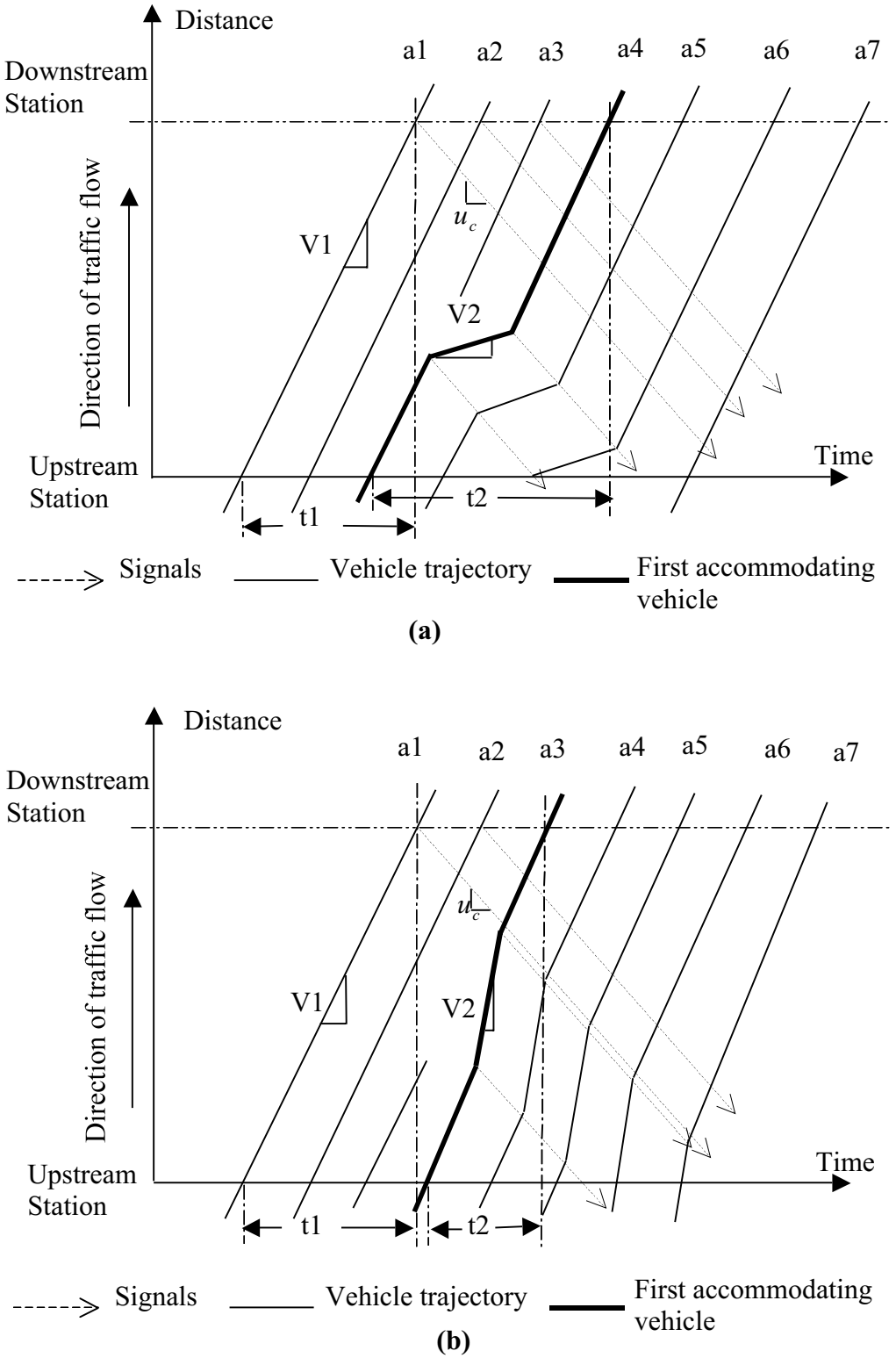

Figure 3-2 Time space diagram showing (a) how an entering vehicle causes delay; (b) how an exiting vehicle reduces delay.

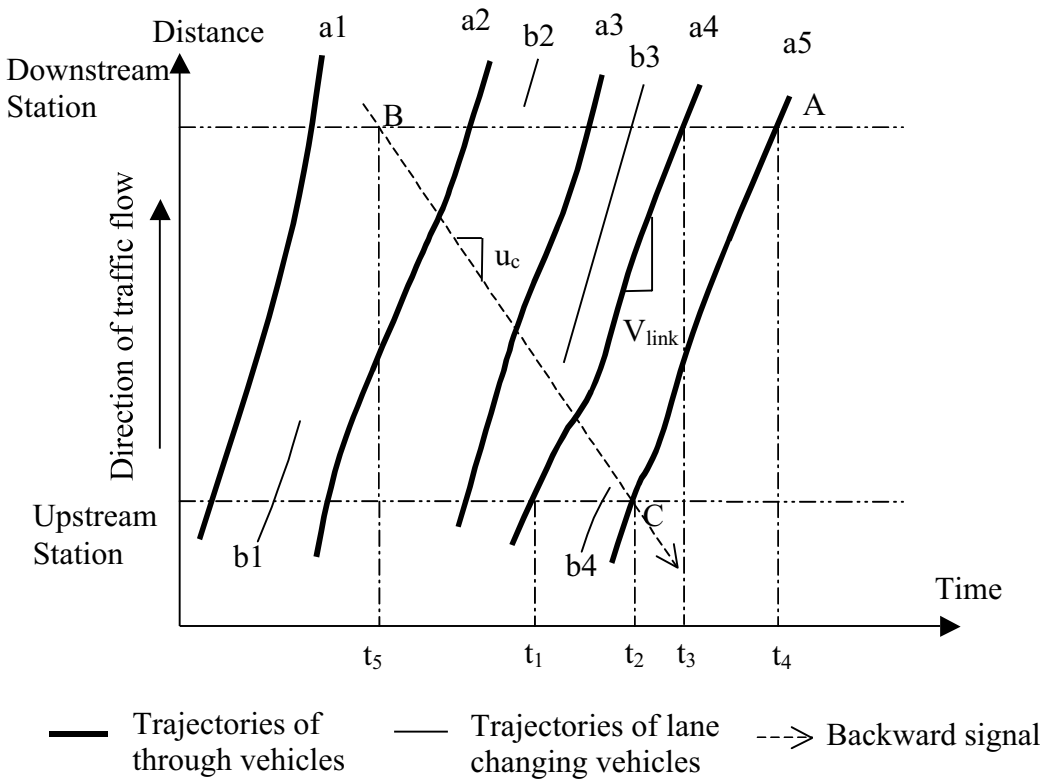

Figure 3-3 Diagram showing the methodology to study the impact of LCMs on delays.

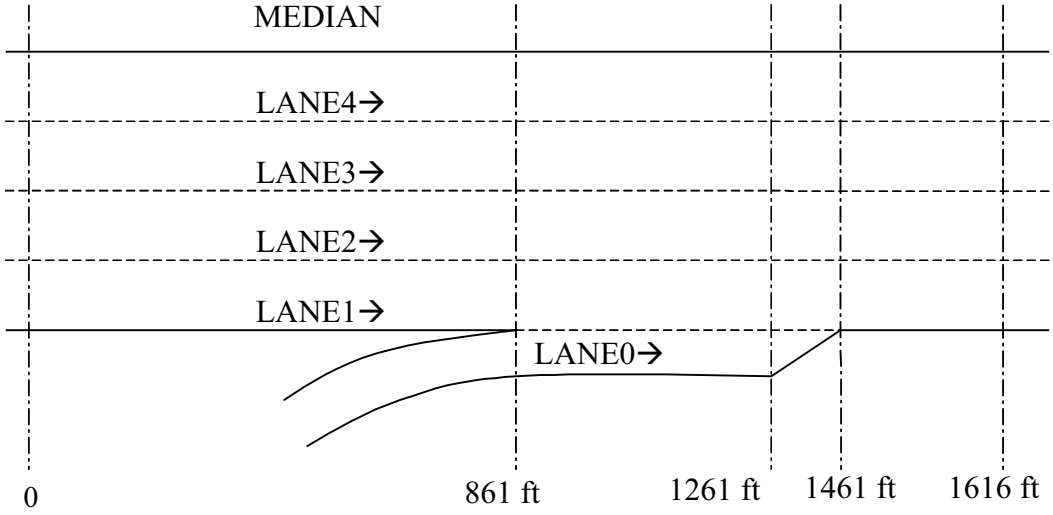

Figure 3-4 Schematic of I-405 section in Los Angeles, not to scale (adapted from Smith, 1985).

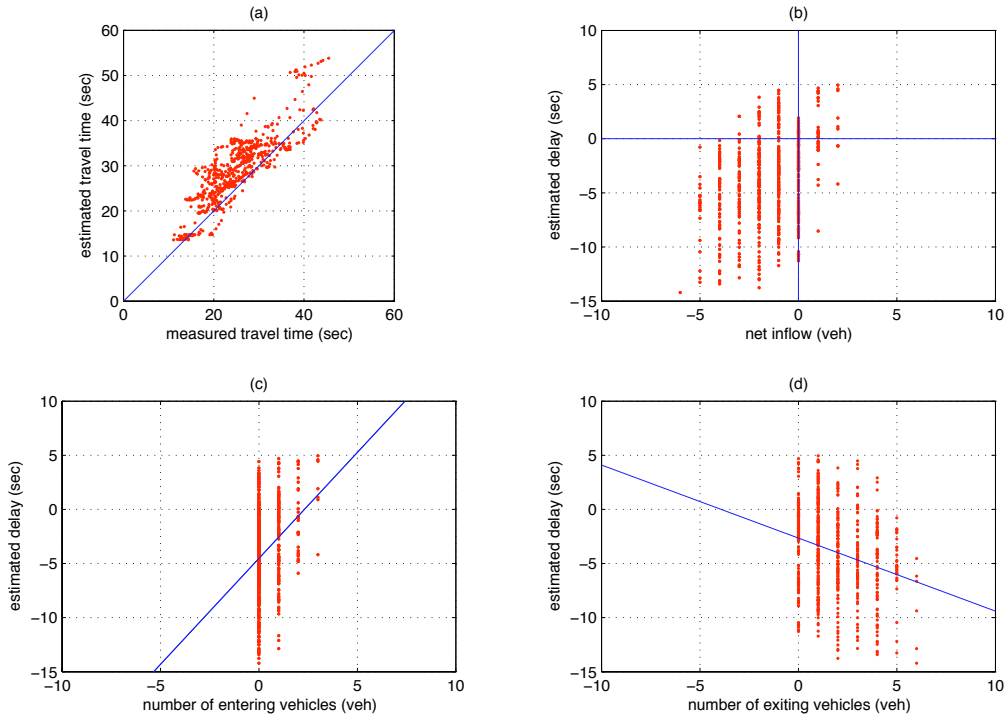

Figure 3-5 Concurrent scatter plots from half hour of I-405 data (a) measured travel time versus estimated travel time; (b) estimated delay versus inflow; (c) estimated delay versus N_{EN}; (d) estimated delay versus N_{EX}.

Table 3-1 Linear Regression Results of three Model Specifications

	Variable	Estimated Coefficient	Standard Error	t-statistic
Model 1	Intercept	-3.21	0.22	-14.35
	N_{EN}	2.19	0.23	9.60
	N_{EX}	-0.78	0.09	-8.49
	No. of observations = 646, $\overline{R}^2$ = 18.3%			
Model 2	Intercept	4.83	0.69	6.96
	N_{EN}	1.55	0.21	7.26
	N_{EX}	-0.84	0.08	-10.11
	K_{dn}	-0.09	0.01	-12.11
	No. of observations = 646, $\overline{R}^2$ = 33.4%			
Model 3	Intercept	2.74	0.60	4.56
	N_{EN}	1.44	0.22	6.45
	N_{EX}	-0.61	0.09	-7.05
	$1/V_{dn}^{a}$	-94.74	8.99	-10.54
	No. of observations = 646, $\overline{R}^2$ = 30.3%			

4 THE EFFECT OF LANE CHANGE MANEUVERS ON A SIMPLIFIED CAR-FOLLOWING THEORY

4.1 Introduction

A recent paper by Newell (2002) proposed a car-following theory based on a very simple rule: namely that during congested periods on a homogeneous highway, the time-space trajectory of a given vehicle is essentially identical to the preceding vehicle's trajectory except for a translation in space and time. This theory uses fewer parameters than its predecessors and provides a new logic to understand car-following phenomena. Because of the simplicity and effectiveness, this theory has rapidly drawn the attentions of several researchers, such as Mauch and Cassidy (2002), Ahn et al. (2004), and Kim and Zhang (2004). The first two papers provide empirical support for Newell's simplified car-following theory from a macroscopic point of view and the latter paper extends this theory to explain the growth or decay of perturbations. Without going into great detail, both Mauch and Cassidy (2002) and Ahn et al. (2004) mentioned that Newell's theory fails in the presence of frequent Lane Change Maneuvers (LCM). Taking a different approach, this section verifies Newell's theory from a microscopic perspective using vehicle trajectory data and it shows that the estimated wave speed according to this theory is consistent with the results from other methods. The present study also reveals clearly the effect of lane change maneuvers on the simple car-following rule proposed by Newell.

This study is organized as follows. First, Newell's car-following theory and subsequent studies are introduced in Section 2. Next, the freeway site used in this study and the trajectory data collected from this site are presented in Section 3. Then the effect of lane change maneuvers on the linear spacing velocity relationship and the verification of Newell's theory based on the trajectory data are presented in Section 4 and Section 5 respectively. Finally, the section closes with a summary and conclusions in Section 6.

4.2 Background

Suppose that on a homogeneous freeway segment, vehicle i is following vehicle $i-1$ and vehicle $i+1$ is following vehicle i, as shown in Figure 4-1A. Vehicle $i-1$ changes velocity from v to v' and its trajectory can be approximated as two straight lines. Based on Newell's theory, during congested periods the trajectory of vehicle i replicates that of vehicle $i-1$ with space shift d_i and time shift τ_i. Furthermore, unlike preceding car-following theories, it is assumed that a driver

follows the preceding vehicle by choosing an appropriate spacing for the current velocity, rather than adjusting velocity after some reaction time.

Newell began his development of the simplified car-following theory from the assumed positive linear relationship between vehicle velocity v and spacing s, which is defined to be the distance between the front ends of two consecutive vehicles. Obviously, drivers tend to choose a larger spacing when the vehicle velocity is increased. However, when vehicle $i-1$ travels at a velocity which is higher than the preferred velocity of driver i, $\hat{V}_i$, driver i will maintain $\hat{V}_i$ and two vehicles will separate. It is assumed that such relationship can be idealized by the linear curve illustrated in Figure 4-1B.

Based on this linear relationship, if driver i travels at velocity v, ($v < \hat{V}_i$), they will choose the spacing as $s_i = s_i^0 + v\mu_i$ and for velocity v', ($v' < \hat{V}_i$), choose spacing $s_i' = s_i^0 + v'\mu_i$. However from Figure 4-1A, it can be easily obtained that

$$s_i = d_i + v\tau_i \tag{4-1A}$$

$$s_i' = d_i + v'\tau_i \tag{4-1B}$$

Comparing these two sets of equations yields $d_i = s_i^0$ and $\tau_i = \mu_i$ if the linear relationship holds. As a result, the wave speed between vehicle $i-1$ and vehicle i is

$$v_w^{i-1,i} = \frac{d_i}{\tau_i} = \frac{s_i^0}{\mu_i} \tag{4-2}$$

and the average wave speed between vehicle $i-1$ and vehicle $i+1$ is

$$v_w^{i-1,i+1} = \frac{d_i + d_{i+1}}{\tau_i + \tau_{i+1}} = \frac{s_i^0 + s_{i+1}^0}{\mu_i + \mu_{i+1}} \tag{4-3}$$

Equations 4-2 and 4-3 imply that the wave speed can be determined by the parameters to describe the relationship between spacing and velocity. A given driver might tend to maintain such a preferred relationship over their trip and the parameters ($s_i^0, \mu_i, \hat{V}_i$) are likely to be different for different drivers. Newell conjectured that [s_i^0, μ_i] will vary as if sampled independently from some

joint probability distribution. So, the wave propagates like a random walk with increment of $[s_i^0, \mu_i]$, which depends on the driving behavior of driver i and is independent of vehicle velocity.

The linear relationship between spacing and velocity is the basic assumption in Newell's theory and it leads to a linear car-following model and a linear relationship between flow and density. If this linear relationship does not hold, based on Equation 4-1, the wave speed between vehicle $i-1$ and vehicle i can be expressed as,

$$v_w = \frac{d_i}{\tau_i} = \frac{s_i' v - s_i v'}{s_i - s_i'} \tag{4-4}$$

Where $s_i = f(v)$ and $f(\bullet)$ is a non-linear function. So, $v_w = g(v, v', f(\bullet))$, that is the wave speed depends on v, v' and the driving behaviors, which is what a non-linear flow density curve would tell us.

Two subsequent papers have validated Newell's theory by studying wave speeds through the traffic stream. Mauch and Cassidy (2002) measured wave trip time on a freeway segment (T) and the number of vehicles through which the wave propagated (N). Based on Newell's theory, $[T, N]$ can be described by a bivariate normal distribution. Two types of segments, with frequent or infrequent lane changing, were studied both in moderately dense queues and very dense incident-induced queues. Despite the traffic condition, the results for all segments marked by infrequent lane changing show that $[T, N]$ on different segments were drawn from a common bivariate normal distribution. However, on segments marked by frequent lane changing, the results for the moderately dense queues fail to support Newell's theory but the results during a very dense queue, arising from an incident, do not show visible discrepancy from Newell's theory. Mauch and Cassidy (2002) explained the former observation with the oscillations induced by lane changing and left detailed explanation for future research.

Ahn et al. (2004) measured the total time (T) and distance (D) covered by a wave arising from long queues discharging at signalized intersections. Vehicle trajectories were constructed and the location of specific velocities was mapped from one trajectory to the next to reveal the propagation of waves. Four waves were studied, which traced vehicle velocity of 0 km/h, 6.5 km/h, 13 km/h and 19.5 km/h. The paper showed that $[s_i^0, \mu_i]$ are independent across drivers and $[T, D]$ for all four observed waves came from the same bivariate normal distribution, which can be characterized by $[s_i^0, \mu_i]$. So, $[s_i^0, \mu_i]$ varied as if they were sampled independently from some joint probability

distribution, as was conjectured by Newell (2002). However, lane change maneuvers were not involved in this study because all cycles in which lane changing was observed were excluded from consideration.

Both papers provided empirical support for Newell's simplified car-following theory by confirming that $[s_i^0, \mu_i]$ for different drivers are independent samples from one common distribution. It was not explicitly shown in either paper that the linear relationship between spacing and velocity is a reasonable assumption. For example, Ahn et al. (2004) looked exclusively at accelerating vehicles, which may deviate from the steady state curve and they sampled only four different vehicle velocities from each vehicle. The effect of lane change maneuvers on Newell's simplified car-following theory was not discussed in detail in either paper.

This present study starts from the microscopic point of view and utilizes vehicle trajectory data to plot the spacing velocity relationship. The results not only support Newell's assumption of linear relationship between spacing and velocity, but also reveal explicitly the effect of lane change maneuvers on Newell's simplified car-following theory.

4.3 Data Description

The present study employed a vehicle trajectory dataset collected by Turner-Fairbank Highway Research Center (TFHRC) in June, 1983 from I-405 South Bound at Santa Monica Blvd., Los Angeles, CA (Smith, 1985). The schematic diagram of the site is shown in Figure 4-2. The site was filmed from a circling aircraft flying at a slow speed. Data were reduced at one frame per second for one hour of the film. Each record contains the information of a vehicle at an instant, which includes vehicle ID, type code, length, speed, lateral and longitudinal position, color code and lane number. Traffic was free flow for the first several minutes, after which a surge in ramp volume caused the average velocity on lane 1 to drop to about 30 km/h and this state continued for the remainder of the dataset. This queuing on lane 1 extend upstream of the section approximately 30 minutes into the film. No incidents affected flow in the section. The second half hour data on lane 1 were selected since our study is focused on the car-following phenomena in congested traffic conditions. Because of the ramp merging activity, the segment after 262 m is marked by frequent lane change maneuvers. To simplify the problem, only the segment between 0 to 244 m (800 feet) is studied. During the second half hour, 796 vehicles entered this 244 m long segment in lane 1, among which 118 vehicles left lane 1 to lane 2 and 31 vehicles entered lane 1 from lane 2. So, about 18% of the vehicles in lane 1 changed lanes.

4.4 The Effect of Lane Change Maneuvers on The Linear Spacing Velocity Relationship

Since the location of each vehicle at each second is known from the trajectory data, it is trivial to calculate the spacing and velocities for each vehicle and plot the relationship as shown in Figure 4-1B. Such trajectory plots are studied in this section to show empirical evidence of the effect of lane change maneuvers. One would expect that lane change maneuvers would disturb the spacing velocity relationship and cause noises in the spacing velocity plots.

4.4.1 Spacing Velocity Relationship for Vehicles Following an Exiting or Entering Vehicle

Suppose that vehicle i in Figure 4-1A leaves the lane, vehicle $i+1$ is then a vehicle following an exiting vehicle. Vehicle $i+1$ will instantly have a large spacing and it may take several seconds for this driver to adjust to their desired spacing for the given velocity. In this accommodation period the observed spacing and velocity might far deviate from the driver's preferred relationship and the period should be treated separately. An example based on vehicle 7922 (TFHRC ID number) is shown in Figure 4-3. Vehicle 7922 was following vehicle 7917 at the beginning of the segment and at time 3260 seconds, vehicle 7917 left lane 1. The 6 observations denoted with triangles in the spacing velocity plot were observed within 6 seconds after the lane change of vehicle 7917. They are defined as *affected points* since these observations are affected by the exiting vehicle and reflect the transient relationship between spacing and velocity during the disturbance. The evolution of the spacing velocity curve shows clearly that after vehicle 7917 left lane 1, vehicle 7922 increased its velocity relative to the new leading vehicle to take advantage of the large spacing left by vehicle 7917 and after 6 seconds (defined as Lane Change Accommodation Time, LCAT), it appears to return to the driver's original spacing velocity relationship. After removing the 6 affected points, the Pearson correlation coefficient between spacing and velocity is increased from 0.54 to 0.87.

A similar analysis can be conducted for the case that vehicle i in Figure 4-1A enters the lane, i.e., vehicle $i+1$ follows an entering vehicle. An example based on vehicle 1560 is shown in Figure 4-4. Vehicle 1557 entered lane 1 before vehicle 1560 at time 600 seconds. Vehicle 1560 decelerated to create a large spacing 4 seconds before this lane change maneuver was recorded in the data set, as shown with the triangles in Figure 4-4, presumably in response to vehicle 1557 beginning to enter lane 1. Vehicle 1560 continued adjusting its spacing and velocity and finally returned to its original spacing velocity relationship 3 seconds after vehicle 1557 changed lanes (denoted as squares in Figure 4-4). The triangles and squares in Figure 4-4 are also defined as *affected points* and LCAT is 7 seconds in this example. After removing the 7 affected points, the Pearson correlation coefficient between spacing and velocity is increased from 0.61 to 0.88.

Relationship plots on other vehicles following existing or entering vehicles also reveal that accommodation to an exiting vehicle is discretionary and to an entering vehicle is mandatory. In other words, if vehicle i forces its way into lane A from lane B, vehicle $i+1$ on lane A has to decelerate immediately to avoid a collision. However, vehicle $i+1$ on lane B does not have to accelerate immediately to take the advantage of large spacing.

LCAT might depend on the driving behavior and traffic conditions, e.g., drivers might tend to fill the gap left by an exiting vehicle quicker in a very dense queue than they might in a moderately dense queue. Explicitly comparing LCAT in different traffic conditions is left to future research.

4.4.2 Spacing Velocity Relationship for Vehicles Changing Lanes

The impact of a lane change maneuver is not limited to the spacing velocity relationship of following vehicles, the maneuver will also likely affect the spacing velocity relationship for the vehicle changing lanes. When a driver undertakes a lane change maneuver, they might be more aggressive or conservative following vehicles in either lane since a key task is to accelerate or decelerate to find an acceptable gap. After completing the lane change maneuver, the driver would then presumably focus strictly on car following, but it might take several seconds to return to their target spacing velocity relationship if the initial spacing deviates from the relationship. We refer to the lane changing vehicle's observations just before and after the lane change as *end points* and the end points are expected to deviate from the driver's typical preferred spacing velocity relationship. An example of entering vehicle is shown in Figure 4-5 and another example of exiting vehicle is shown in Figure 4-6.

In Figure 4-5, vehicle 8586 entered lane 1 from lane 2 at time 3524 seconds and then followed vehicle 8583. The 6 observations denoted with circles in the spacing velocity plot were observed within 6 seconds after the lane change maneuver. They show that vehicle 8586 had relatively high velocity and low spacing immediately after entering lane 1. After that, the observations show the pattern similar to what is assumed by Newell (2002). There are two observations far from the preferred relationship at time about 3543 seconds (denoted with "+" in Figure 4-5) which appear to be due to a backward moving acceleration wave. After removing the 6 end points, the Pearson correlation coefficient between spacing and velocity is increased from 0.16 to 0.70.

In Figure 4-6, vehicle 5471 left lane 1 at time 2268 seconds, 3 seconds before this lane change maneuver, vehicle 5471 accelerated and the observations deviated from the rest of the observed spacing velocity relationship.

4.4.3 Spacing Velocity Relationship for Many Lane Change Maneuvers

Extending the analysis to all 118 vehicles left lane 1 to lane 2 and 31 vehicles that entered lane 1 from lane 2, we were able to extract relationships shown in Figures 4-3 through 4-6 for approximately 62 percent of the vehicles. The remaining vehicles were excluded either due to the fact that multiple successive maneuvers overlapped or because the range exhibited in the spacing-velocity plane was too small to distinguish between noise and the impacts of lane change maneuvers. Figure 4-7 shows the Cumulative Distribution Function (CDF) of the LCAT from the four cases. The sample size of each group is shown in parentheses in the legend.

As with the individual examples presented earlier, vehicles following an exiting vehicle tend to have a larger accommodation time than those behind an entering vehicle (discretionary versus mandatory accommodation). The CDF of LCAT from entering vehicles is very similar to that of vehicles following them. For this data set the median LCAT for entering vehicles and vehicles following entering vehicles is 3 sec faster than the median LCAT for vehicles following exiting vehicles. One should also note that the accommodation by an entering vehicle and following vehicle are concurrent rather than successive, e.g., vehicle 1560 and vehicle 1557 in Figure 4-4 accommodate the lane change maneuver over the same time period.

4.5 Verification of The Linear Spacing Velocity Relationship

A hypothesis test was used to check whether a linear relationship exists between spacing and velocity for each vehicle in the study set. The hypothesis is,

$$H_0 : r = 0$$

$$H_A : r \neq 0$$

where r is the Pearson correlation coefficient between spacing and velocity.

In this study, 796 vehicles were originally observed on lane 1. However, the spacing velocity plots for 27 vehicles have 10 or fewer observations and 236 vehicles had velocities spanning less than 16 km/h (10 mph). In either case, the data do not show sufficient range to suppress measurement noise in the spacing velocity relationship and these 263 vehicles are excluded from further analysis. It is not be surprising to remove observations for so many vehicles because the 250 meter long segment limited the duration a given vehicle was observed. The remaining set consists of 533 vehicles and the hypothesis test was conducted for each of these remaining vehicles. The result showed that 465

out of 533 hypothesis tests resulted in P-values smaller than 0.05. So, about 87% of the hypothesis tests would result in rejection of the null hypothesis if they were tested at 5% significance level.

The Pearson correlation coefficient measures the strength and direction of the linear relationship between two variables. The bigger the coefficient is, the stronger the two variables are linearly related. To see the strength of this linear relationship, the Pearson correlation coefficient between spacing and velocity was calculated for each of the 533 vehicles. The CDF across these correlation calculations is plotted in Figure 4-8.

About 45% of the vehicles show a correlation of spacing and velocity higher than 0.80 and about 70% of the vehicles show a correlation higher than 0.60. Considering that these results are based on vehicle trajectories on a segment about 250 meters long and some noise is likely to still be present, Figure 4-8 suggests that the linear relationship between spacing and velocity assumed by Newell (2002) is reasonable for many of the vehicles. Note that this set includes all observations influenced by lane change maneuvers, e.g., affected points in Figures 4-3 and 4-4 and end points in Figures 4-5 and 4-6 were not removed and account for some of the low correlations.

A linear regression was applied to the observations from each of the 533 vehicles and one set of $[s_i^0, \mu_i]$ was obtained for each regression. Based on Equation 4-3, the average wave speed through the segment is the quotient of the sum of s_i^0 and the sum of μ_i. The mean s_i^0, μ_i and the estimated average wave speed are shown in Table 4-1.

The results in Table 4-1 are similar to the results shown in Ahn et al. (2004), which were estimated with maximum likelihood. Wang et al. (2004) proposed two methods, Cross Correlation Analysis and Cross Spectral Analysis, to estimate wave speed based on velocity observations at two discrete points in space. Both methods were applied on the subject dataset and the estimated wave speeds are 17.33 km/h and 16.46 km/h, respectively. These results are consistent with the wave speed estimation shown in Table 4-1.

4.6 Conclusions

Newell (2002) proposed a simple car following theory that used fewer parameters and a novel logic. An important assumption for this theory is that the relationship between spacing and velocity for a single vehicle can be approximated by a piecewise linear curve, which directly leads to Newell's linear car following theory and the conclusion that waves propagate like a random walk. Two subsequent papers have validated Newell's theory by showing that the intercept and slope of the linear spacing velocity relationship vary as if they are drawn independently from a joint distribution.

These papers explicitly verified the random walk property of the waves and the independence of wave speed to vehicle velocities. However, it was not shown explicitly how reasonable the linear spacing velocity relationship is. In addition, although both papers mentioned that Newell's theory fails in the presence of frequent lane change maneuvers, no detailed analysis of the effect of lane change maneuvers were presented.

This section studied spacing velocity relationship from vehicle trajectory data. Using several examples it was shown that a given lane change maneuver not only perturbs the spacing velocity relationship of following vehicles, but also perturbs the spacing velocity relationship of the vehicle making the maneuver. Namely, the large spacing left by an exiting vehicle or the small spacing caused by an entering vehicle will induce a transient deviation from the normally preferred relationship. Although the preferred spacing velocity relationship recovers from such a perturbation, the observations during LCAT will differ from other times. On the other hand, when a vehicle changes lanes the driver might not follow their normal driving behavior and thus, cause other deviations from the spacing velocity relationship. Obviously, the smaller the impact caused by lane change maneuvers, the better Newell's theory can describe macroscopic traffic behavior. For example, Mauch and Cassidy (2002) observed that Newell's theory seemed inappropriate for a moderately dense queue but reasonable for a very dense queue induced by an incident, both were marked by frequent lane change maneuvers. Their observation may be explained if it can be shown that the preferred spacing velocity relationship can recover sooner from the perturbations induced by lane change maneuvers in a very dense queue than in a moderately dense queue, but such proofs are left to future research.

The Pearson correlation coefficients between spacing and velocity for 533 vehicles were calculated and the hypothesis tests were conducted. The results show that the assumption of the linear relationship between spacing and velocity is reasonable most of the time for study sample. The calculated $[s_i^0, \mu_i]$ and estimated average wave speed are consistent with earlier empirical studies. In other words, these results provide evidence that Newell's simplified model appears to capture the dominant preferences of drivers. However, dynamic events can cause significant deviations from this static curve, such as the lane change maneuvers in Figures 4-3 and 4-4. Provided the dynamic events are relatively infrequent, the static state would be expected to dominate average conditions.

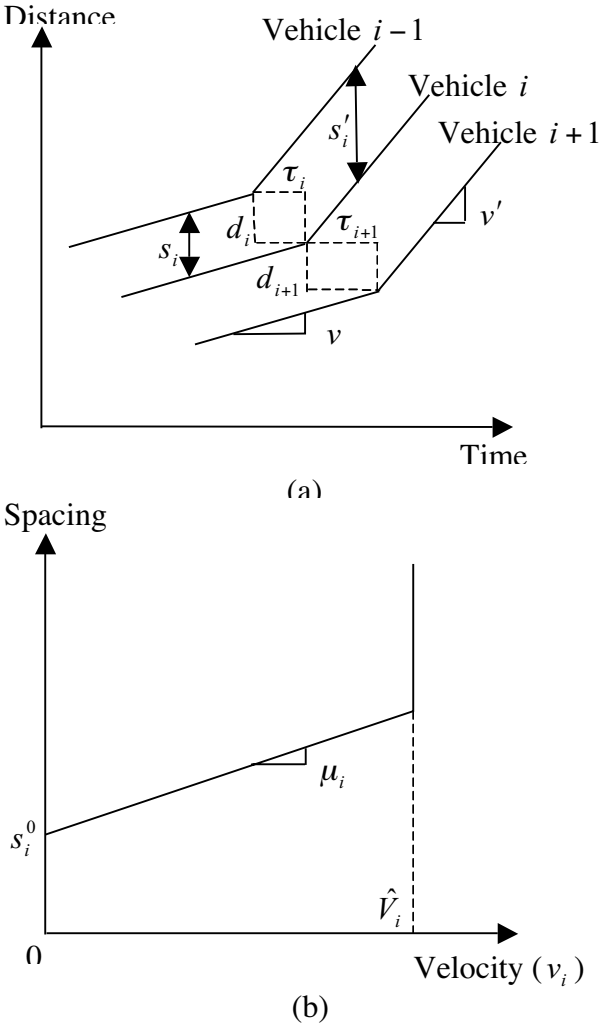

Figure 4-1 (a) Piecewise linear approximation to vehicle trajectories; (b) Relationship between spacing and velocity for an individual vehicle (adapted from Newell, 2002).

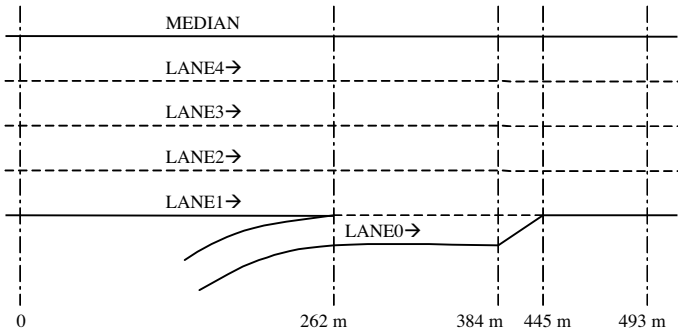

Figure 4-2 Schematic of I-405 section in Los Angeles, not to scale (adapted from Smith, 1985).

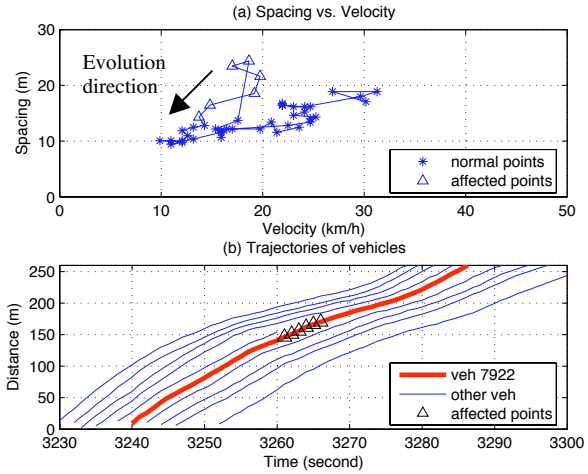

Figure 4-3 (a) Spacing velocity plot of vehicle 7922 (following exiting vehicle 7917), and (b) the corresponding vehicle trajectories.

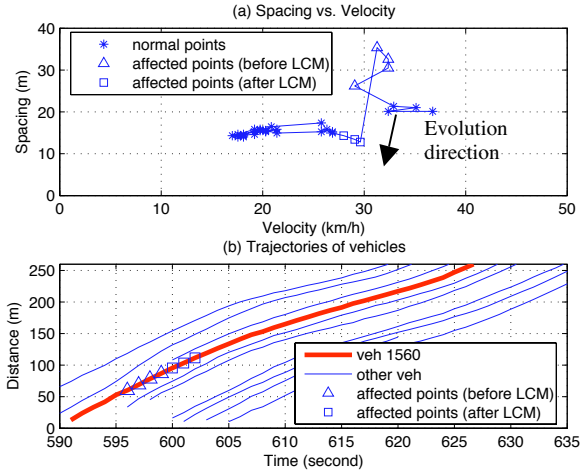

Figure 4-4 (a) Spacing velocity plot of vehicle 1560 (following entering vehicle 1557), and (b) the corresponding vehicle trajectories.

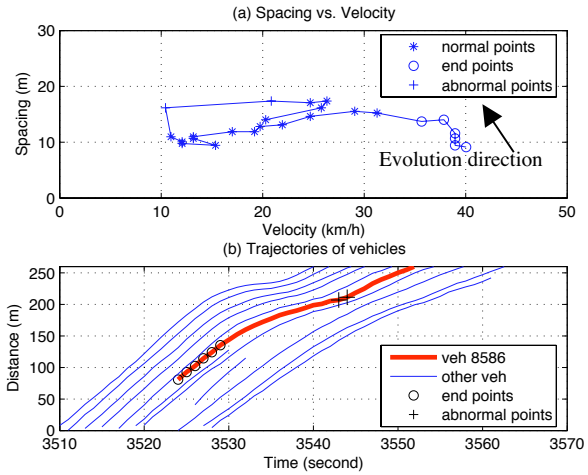

Figure 4-5 (a) Spacing velocity plot of an entering vehicle (8586), and (b) the corresponding vehicle trajectories.

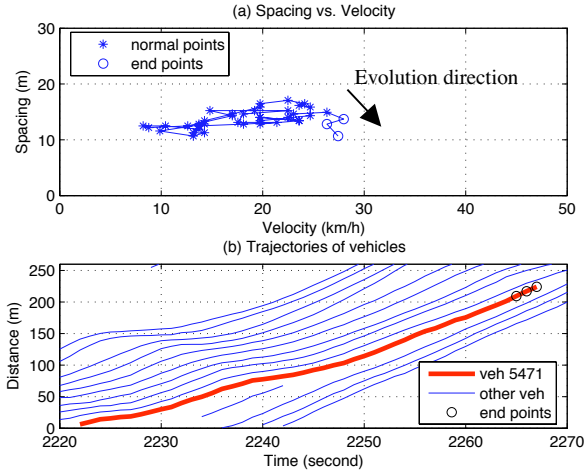

Figure 4-6 (a) Spacing velocity plot of an entering vehicle (8586), and (b) the corresponding vehicle trajectories.

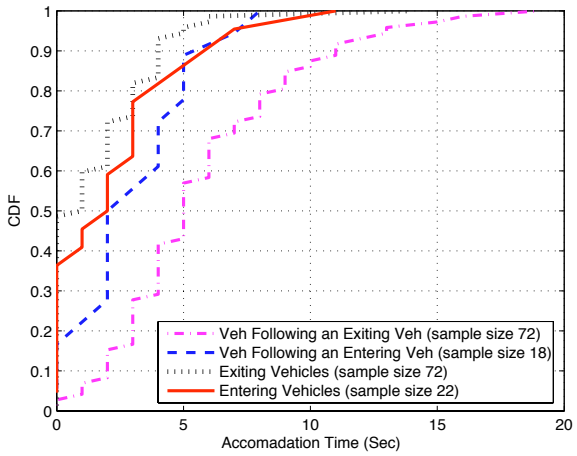

Figure 4-7 CDF of Lane Change Accommodation Time from four cases.

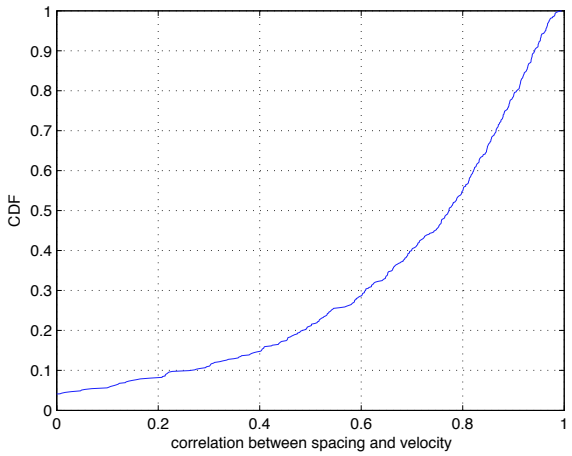

Figure 4-8 CDF of the correlation between spacing and velocity.

Table 4-1 The Result of Wave Speed Estimation Based on Newell's Theory

$\bar{s}^0$ (m)	$\bar{\mu}$ **(seconds)**	**Estimated average wave speed (km/h)**
6.90	1.36	18.30

5 CONCLUSIONS

Conventional vehicle detectors are capable of monitoring discrete points along the roadway but do not provide information about conditions on the link between detectors. Section 2 developed a robust vehicle reidentification algorithm to quantify conditions between detector stations. The distinct vehicles were key to this reidentification, namely the long vehicles in this case.

The reidentification results were used to find link travel times until link velocity dropped below 20 mph. About 40 percent of long vehicles were consistently reidentified over links on the order of 1 mi long using dual loop detector data, and a slightly lower reidentification rate when using single loop detector data. The travel time measurements obtained from the reidentified vehicles will be useful for studying the traffic conditions in the freeways. This work advances our earlier efforts significantly. First, the ability to match vehicles between single loop detector stations opens up additional roadways for analysis. But the most important contribution of the new algorithm is the fact that the present research does not limit vehicle reidentification to only one lane, which allows vehicle reidentification even when the candidate vehicle changes lanes. The improved detection allows for reidentification across major merges or diverges in the freeway segment, where one cannot assume that most vehicles travel along the same lane. Two out of the three links examined included a major merge and major diverge of two interstate freeways. The examples include a case where the reidentification algorithm responded to delay between two detector stations an hour before the delay was locally observable at either of the stations used for reidentification.

This analysis can be used to provide recommendations on future funding decisions for investment on expensive new infrastructure for travel time measurement, focusing resources only on freeways that promise to show an improvement in operations due to provision of travel time information. The new information would be useful to the operating agencies for taking timely decisions in response to various delay causing events and hence reduce the resulting congestion of the system. Finally, although the research uses loop detector data, it would be equally applicable to data obtained from any other traffic detector that provides a reproducible vehicle feature.

Section 3 presents the concept of delay caused by LCMs and proposes a method to estimate it. The estimation result is further applied to study the impact of LCMs on delays using trajectory data. Such study should help understand traffic delay for better congestion management and further the understanding of traffic dynamics into an important area where much remains unknown. A pilot study shows that the proposed study methods are feasible. Nevertheless, further research needs to be carried out to evaluate the impact of some of the simplifying assumptions made. Several linear

regression models from this pilot study are presented and the results comply with the expectations. Section 3 provides an empirical start for the study of LCMs impacts on delay.

There are some limitations of the work that should be addressed in the future, several of which are as follows. The proposed methodology has so far been tested only on half-hour of trajectory data from a single lane on a section just before an on-ramp. The observation data at the simulated upstream and downstream stations are interpolated from the vehicle trajectories, rather than collected from the field. In addition, the inhomogeneous geometric features of this section might have caused the low goodness-of-fit measure of the linear regression models. Identifying the impacts of inhomogeneous features is an important topic for further research and trajectory data collected from congested traffic conditions are necessary for further study.

Several assumptions and simplifications are made in section 3 and some of them need further verification treatment. The wave velocity was assumed to be constant, a value of 10 mph was used in the pilot study. Although not shown in this report, the value of the constant wave velocity was proven to be an important confounding factor and its value should be determined carefully, as was done herein with five different methods. In addition, this study counts the number of LCMs in the triangular time space region as ABC shown in Figure 3-3. However, this triangular region is just a simplification since some LCMs outside of this region might also contribute to the delay. For example, vehicle b4 in Figure 3-3 will not influence the travel time of vehicle a5 between the two stations and will not contribute to the delay of vehicle a5 if it is assumed that a vehicle can change its speed instantly. However, in reality vehicle a5 will need some time to accommodate the lane change of vehicle b4 and such accommodation might occur between the two stations if vehicle b4 changes lane at a spot that is very close to the line BC in Figure 3-3. Given that the numbers of entering and exiting vehicles are discrete variables, the treatment of such explanatory variables in statistically modeling delay relationships requires further attention.

One needs to both understand the operation of individual lanes and the combination of all lanes in a given direction. Section 3 is limited to the former, when considering the impacts across all lanes. On the one hand, it remains possible that some of the effects may cancel out and become imperceptible in aggregate delay. On the other hand, an aggregate delay could still be present and detectable due to the finding in this section that the delay caused by a LCM into a lane is greater than the gain in travel time resulting from a LCM out of a lane. Moreover, because the accommodation occurs over long distances, the gain in one lane may be spatially or temporally separated from the loss in another. Although this imbalance may be small, it could prove to be one mechanism that causes delay and disturbances (e.g., the driver behind an entering vehicle may decelerate and then accelerate to accommodate the LCM, all following vehicles will be constrained by the fluctuations in this

trajectory as the impacts propagate upstream). Likewise, a vehicle momentarily consumes more capacity while straddling two lanes than it would have had it remained in a single lane. From a capacity and delay standpoint one may argue that these phenomena are only important within a bottleneck, which may prove to be true, but the understanding of LCMs within a queue should also further understanding LCMs' impacts within a bottleneck where they can impact throughput. The understanding could also lead to establishing more precisely the influence area of a bottleneck, where it begins and ends. Away from bottlenecks the work potentially has implications on safety (e.g., accidents due to stop and go traffic) and car following theory. Finally, if LCMs away from a bottleneck cause a measurable change in delay for a given lane, it could provide a tool to quantify LCMs within a queue even if LCMs do not impact the net delay across all lanes, thereby providing previously unavailable details about the flow of vehicles within a queue.

Newell (2002) proposed a simple car following theory that used fewer parameters and a novel logic. An important assumption for this theory is that the relationship between spacing and velocity for a single vehicle can be approximated by a piecewise linear curve, which directly leads to Newell's linear car following theory and the conclusion that waves propagate like a random walk. Two subsequent papers have validated Newell's theory by showing that the intercept and slope of the linear spacing velocity relationship vary as if they are drawn independently from a joint distribution. These papers explicitly verified the random walk property of the waves and the independence of wave speed to vehicle velocities. However, it was not shown explicitly how reasonable the linear spacing velocity relationship is. In addition, although both papers mentioned that Newell's theory fails in the presence of frequent lane change maneuvers, no detailed analysis of the effect of lane change maneuvers were presented.

Section 4 studied spacing velocity relationship from vehicle trajectory data. Using several examples it was shown that a given lane change maneuver not only perturbs the spacing velocity relationship of following vehicles, but also perturbs the spacing velocity relationship of the vehicle making the maneuver. Namely, the large spacing left by an exiting vehicle or the small spacing caused by an entering vehicle will induce a transient deviation from the normally preferred relationship. Although the preferred spacing velocity relationship recovers from such a perturbation, the observations during LCAT will differ from other times. On the other hand, when a vehicle changes lanes the driver might not follow their normal driving behavior and thus, cause other deviations from the spacing velocity relationship. Obviously, the smaller the impact caused by lane change maneuvers, the better Newell's theory can describe macroscopic traffic behavior. For example, Mauch and Cassidy (2002) observed that Newell's theory seemed inappropriate for a moderately dense queue but reasonable for a very dense queue induced by an incident, both were marked by frequent lane change maneuvers. Their observation may be explained if it can be shown that the preferred spacing

velocity relationship can recover sooner from the perturbations induced by lane change maneuvers in a very dense queue than in a moderately dense queue, but such proofs are left to future research.

The Pearson correlation coefficients between spacing and velocity for 533 vehicles were calculated and the hypothesis tests were conducted. The results show that the assumption of the linear relationship between spacing and velocity is reasonable most of the time for study sample. The calculated [s_i^0, μ_i] and estimated average wave speed are consistent with earlier empirical studies. In other words, these results provide evidence that Newell's simplified model appears to capture the dominant preferences of drivers. However, dynamic events can cause significant deviations from this static curve, such as the lane change maneuvers in Figures 4-3 and 4-4. Provided the dynamic events are relatively infrequent, the static state would be expected to dominate average conditions.

6 ACKNOWLEDGMENTS

The author would like to acknowledge the input, contributions and support from Rabi Mishalani, Chao Wang, and Sivaraman Krishnamurthy at the Ohio State University. This report includes their input and comments.

7 REFERENCES

Ahmed K.I., Ben-Akiva M., Koutsopoulos H.N. and Mishalani R.G., (1996). "Models of freeway lane changing and gap acceptance behavior." *Proceedings of the 13th International Symposium on Transportation and Traffic Theory*, Lyon, France.

S. Ahn, M. J. Cassidy and J. Laval, (2004). "Verification of a simplified car-following theory," *Transportation Research Part B*, vol. 38, no. 5, pp. 431-440.

Banks, J. H., (1989). "Freeway speed-flow concentration relationships: more evidence and interpretations." *Transportation Research Record, No. 1225*, pp. 53-60.

Coifman, B., (1998). "Vehicle reidentification and travel time measurement in real-time on freeways using the existing loop detector infrastructure," *Transportation Research Record, No. 1643*, pp. 181-191.

Coifman, B., Lyddy, D., Skabardonis, A., (2000). "The Berkeley Highway Laboratory- Building on the I-880 Field Experiment", *Proc. IEEE ITS Council Annual Meeting*, pp 5-10.

Coifman, B. (2002). "Estimating travel times and vehicle trajectories on freeways using dual loop detectors." *Transportation Research Part A*, Vol. 36, No. 4, pp. 351-364.

Coifman, B. and Cassidy, M., (2002). "Vehicle reidentification and travel time measurement on congested freeways." *Transportation Research Part A*, Vol. 36, Issue 10, pp. 899-917.

Coifman, B., (2003). "Identifying the Onset of Congestion Rapidly with existing Traffic Detectors," *Transportation Research Part A*, Vol 37 Issue 3, pp 277-291

Coifman, B., Dhoorjaty, S., Lee, Z., (2003a). "Estimating Median Velocity instead of Mean Velocity at Single Loop Detectors", *Transportation Research Part C*, Vol 11, Issue 3-4, pp 211-222

Coifman, B., Krishnamurthy, S., and Wang, X., (2003b). "Lane Change Maneuvers Consuming Freeway Capacity", *Proc. of the Traffic and Granular Flow 2003 Conference*, October 3, Delft, Netherlands, pp. 3-14.

Coifman, B. and Wang, Y., (2005). "The Velocity of Waves Propagating Through Congested Freeway Traffic," *Proc. of The 16th International Symposium on Transportation and Traffic Theory*, July 19-21, College Park, MD, pp. 165-179.

Cassidy, M.J., (1998). "Bivariate relations in nearly stationary highway traffic." *Transportation Research Part B*, Vol. 32, pp. 49-59.

Cassidy, M.J. and Mauch, M., (2001). "An observed feature of long freeway traffic queues." *Transportation Research Part A*, Vol. 35, pp. 143-156.

Edie, L., (1963). "Discussion of traffic stream measurements and definitions," *Proc. Second International Symposium on the Theory of Traffic Flow*, OECD, Paris, France, 1963, pp. 139-154.

Hall, F. L. and Gunter, M. A., (1986). "Further analysis of the flow-concentration relationship." *Transportation Research Record, No. 1091*, pp. 1-9.

Hellinga, B., (2001). "Automated vehicle identification tag-matching algorithms for estimating vehicle travel times: comparative assessment." *Transportation Research Record, No. 1774*, pp. 106-114.

Hidas P., (2002). "Modelling lane changing and merging in microscopic traffic simulation." *Tranportation Search Part C*, Vol. 10C, pp. 351-371.

Huang, T., Russell, S., (1997). "Object Identification in a Bayesian Context", *Proc. the Fifteenth International Joint Conference on Artificial Intelligence* (IJCAI-97), Nagoya, Japan. Morgan Kaufmann.

Izumi, T., Takahashi, Y. and Kiryu, N., (2000). "Travel time measurement using ultrasonic vehicle-identification equipment." *The Transactions of the Institute of Electrical Engineers of Japan*, Vol. 120D, pp. 651-657.

Gazis D. C., Herman R., and Weiss G. H.,(1962). "Density oscillations between lanes of multilane highways." *Operations Res.*, Vol. 10, No.5, pp. 658-667.

Gipps P.G., (1986) "A model for the structure of lane-changing decisions." *Transportation Research Part B*, Vol. 20B, No. 5, pp. 403-414.

Jain, M., Coifman, B., (2005). "Improved Speed Estimates from Freeway Traffic Detectors" *ASCE Journal of Transportation Engineering*, Vol 131, No 7, 2005, pp483-495.

T. Kim and H. M. Zhang. (2004). "Gap time and stochastic wave propagation," in *2004 IEEE Intelligent Transportation Systems Conference*, Washington DC, USA, pp. 88-93.

Kuhne, R., Immes, S., (1993). "Freeway Control Systems for Using Section-Related Traffic Variable Detection," *Proc. of Pacific Rim TransTech Conference*, Vol 1, ASCE, pp 56-62.

MacCarley, A.C., (1998). *Videobased Vehicle Signature Analysis and Tracking Phase1: Verification of Concept and Preliminary Testing*. California PATH Working Paper, UCB-ITS-PWP-98-10.

MacCarley, A.C., (2001). *Video-based Vehicle Signature Analysis and Tracking System Phase 2: Algorithm Development and Preliminary Testing*, California PATH Working Paper, UCB-ITS-PWP-2001-10

Mauch, M. and Cassidy, M.J., (2002). "Freeway traffic oscillations: observations and predictions." *Proceedings of the 15th International Symposium on Transportation and Traffic Theory*, Elsevier, Amsterdam, pp. 653-674.

Michalopoulos P., Beskos D., and Yamauchi Y., (1984). "Multilane traffic flow dynamics: Some macroscopic considerations." *Transportation Research*, 18B, pp. 377-393.

Munjal P.K. and Pipes L.A., (1971). "Propagation of on-ramp density waves on non-uniform unidirectional two-lane freeways. *Transportation Research*, Vol. 5, pp. 241-255.

Neelisetty, S., Coifman, B., (2004). "Improved Single Loop Velocity Estimation in the Presence of Heavy Truck Traffic," *Proc. of the 83rd Annual Meeting of the Transportation Research Board.*

Newell, G.F., (1993). "A simplified theory of kinematic waves in highway traffic, part II: queuing at freeway bottlenecks," *Transportation Research Part B*, Vol. 27, pp. 289-303.

Newell, G.F., (2002). "A simplified car-following theory: a lower order model," *Transportation Research Part B*, Vol. 36, pp. 195-205.

Sheu J-B., (1999). "A stochastic modeling approach to dynamic prediction of section-wide inter-lane and intra-lane traffic variables using point detector data." *Transportation Research Part A*, Vol. 33A, pp. 79-100.

Sheu J-B. and Ritchie S.G., (2001) "Stochastic modeling and real-time prediction of vehicular lane-changing behavior." *Transportation Research Part B*, Vol. 35B, pp. 695-716.

Smith, S.A., (1985). *Freeway Data Collection for Studying Vehicle Interactions*, Technical Report, Report No. FHWA/RD-85/108.

Toledo T., Koutsopoulos H.N. and Ben-Akiva M.E., (2003). "Modeling integrated lane-changing behavior." *Transportation Research Record, No. 1857*, pp. 30-38.

Wang, Y., Foster, D. and Coifman, B., (2004). "Measuring wave velocities on highways during congestion using cross spectral analysis." *2004 IEEE Intelligient Transportation Systems Conference*, Washingtong, D.C., pp. 544-547.

Wei H., Meyer E., Lee J. and Feng C., (2000). "Characterizing and modeling observed lane-changing behavior." *Transportation Research Record, No. 1710*, pp. 104-113.

Windover, J. and Cassidy, M., (2001). "Some observed details of freeway traffic evolution." *Transportation Research Part A*, Vol. 35, pp. 881-894.

Worrall R. D., Bullen A. G., and Gur Y., (1970) "An elementary stochastic model of lane-changing on a multilane highway." *Highway Res. Rec.*, 308, pp. 1-12.

Yang Q. and Koutsopoulos H.N., (1986). "A microscopic traffic simulator for evaluation of dynamic traffic management systems." *Transportation Research Part C*, Vol 4C, No. 3, pp. 113-129.

Zhang Y., Owen L.E. and Clark J.E., (1998). "Multiregime approach for microscopic traffic simulation." *Transportation Research Record, No. 1644*, pp. 103-115.